

# UCLA

## UCLA Previously Published Works

### Title

IL-10 promotes endothelial progenitor cell infiltration and wound healing via STAT3

### Permalink

<https://escholarship.org/uc/item/3653c5n8>

### Journal

The FASEB Journal, 36(7)

### ISSN

0892-6638

### Authors

Short, Walker D

Steen, Emily

Kaul, Aditya

et al.

### Publication Date

2022-07-01

### DOI

10.1096/fj.201901024rr

### Copyright Information


This work is made available under the terms of a Creative Commons Attribution-NonCommercial-NoDerivatives License, available at

<https://creativecommons.org/licenses/by-nc-nd/4.0/>

Peer reviewed

## RESEARCH ARTICLE

# IL-10 promotes endothelial progenitor cell infiltration and wound healing via STAT3

Walker D. Short<sup>1</sup> | Emily Steen<sup>1</sup> | Aditya Kaul<sup>1</sup> | Xinyi Wang<sup>1</sup> | Oluyinka O. Olutoye II<sup>1</sup> | Hima V. Vangapandu<sup>1</sup> | Natalie Templeman<sup>1</sup> | Alexander J. Blum<sup>1</sup> | Chad M. Moles<sup>1</sup> | Daria A. Narmoneva<sup>2</sup> | Timothy M. Crombleholme<sup>3,4</sup> | Manish J. Butte<sup>5</sup> | Paul L. Bollyky<sup>6</sup> | Sundeep G. Keswani<sup>1</sup> | Swathi Balaji<sup>1</sup> 

<sup>1</sup>Division of Pediatric Surgery, Department of Surgery, Texas Children's Hospital and Baylor College of Medicine, Houston, Texas, USA

<sup>2</sup>Biomedical Engineering, Department of Biomedical, Chemical and Environmental Engineering, College of Engineering and Applied Sciences, University of Cincinnati, Cincinnati, Ohio, USA

<sup>3</sup>Division of Pediatric General Thoracic and Fetal Surgery, Connecticut Children's Hospital, University of Connecticut School of Medicine, Farmington, Connecticut, USA

<sup>4</sup>Fetal Care Center Dallas, Dallas, Texas, USA

<sup>5</sup>Division of Immunology, Allergy, and Rheumatology, Departments of Pediatrics and Microbiology, Immunology, and Molecular Genetics, University of California Los Angeles, Los Angeles, California, USA

<sup>6</sup>Division of Infectious Diseases, Department of Medicine, Stanford University School of Medicine, Stanford, California, USA

## Correspondence

Swathi Balaji, Division of Pediatric Surgery, Department of Surgery, Texas Children's Hospital and Baylor College of Medicine, Feigin Center, C.450.05, 1102 Bates Avenue, Houston, TX 77030, USA.

Email: [balaji@bcm.edu](mailto:balaji@bcm.edu)

## Funding information

NIGMS, Grant/Award Number: 1R01GM111808NIH; Wound Healing Society Foundation, Grant/Award Number: 3M Award; Gulf Coast Consortia, Grant/Award Number: John S. Dunn Foundation Collaborative Research Award

## Abstract

Endothelial progenitor cells (EPCs) contribute to de novo angiogenesis, tissue regeneration, and remodeling. Interleukin 10 (IL-10), an anti-inflammatory cytokine that primarily signals via STAT3, has been shown to drive EPC recruitment to injured tissues. Our previous work demonstrated that overexpression of IL-10 in dermal wounds promotes regenerative tissue repair via STAT3-dependent regulation of fibroblast-specific hyaluronan synthesis. However, IL-10's role and specific mode of action on EPC recruitment, particularly in dermal wound healing and neovascularization in both normal and diabetic wounds, remain to be defined. Therefore, inducible skin-specific STAT3 knockdown mice were studied to determine IL-10's impact on EPCs, dermal wound neovascularization and healing, and whether it is

**Abbreviations:** 4-OHT, 4-hydroxy tamoxifen; ΔΔCt, comparative Ct; AFB, adult fibroblasts; ANOVA, analysis of variance; BGS, Bovine growth serum; BM, bone marrow; CD133, cluster of differentiation 133 molecule (also known as Prominin1); CD34, cluster of differentiation 34 molecule; CXCL12, C-X-C motif chemokine 12; CXCR4, C-X-C chemokine receptor type 4; DMEM, Dulbecco's modified Eagle's media; ECL, enhanced chemoluminescence; ECM, extracellular matrix; ECs, endothelial cells; ELISA, enzyme-linked immunosorbent assay; EPCs, endothelial progenitor cells; FLK-1, fetal liver kinase 1 (also known as KDR, is a receptor for VEGF); GFP, green fluorescent protein; H&E, hematoxylin and eosin; HIF-1, hypoxia inducible factor 1; HSCs, hematopoietic stem cells; IgG, immunoglobulin G; IHC, immunohistochemistry; IL-10, interleukin 10; IL-10R, interleukin 10 receptor; LV-GFP, Lenti virus expressing GFP; LV-IL-10, Lenti virus expressing IL-10; MI, myocardial infarction; PBS, phosphate buffered saline; PSF, penicillin, streptomycin, amphotericin; p-STAT3, phosphorylated signal transducer and activator of transcription 3; qPCR, real time-polymerase chain reaction; SDF-1α, stromal cell-derived factor 1α; shRNA, short hairpin RNA; STAT3, signal transducer and activator of transcription 3; TBS, Tris-buffered saline; TGF-β1, β3, transforming growth factor-β1, β3; Tween-20, polysorbate-20; VEGF, vascular endothelial growth factor.

This is an open access article under the terms of the [Creative Commons Attribution-NonCommercial-NoDerivs](https://creativecommons.org/licenses/by-nc-nd/4.0/) License, which permits use and distribution in any medium, provided the original work is properly cited, the use is non-commercial and no modifications or adaptations are made.

© 2022 The Authors. *The FASEB Journal* published by Wiley Periodicals LLC on behalf of Federation of American Societies for Experimental Biology.

STAT3-dependent. We show that IL-10 overexpression significantly elevated EPC counts in the granulating wound bed, which was associated with robust capillary lumen density and enhanced re-epithelialization of both control and diabetic (db/db) wounds at day 7. We noted increased VEGF and high C-X-C motif chemokine 12 (CXCL12) levels in wounds and a favorable CXCL12 gradient at day 3 that may support EPC mobilization and infiltration from bone marrow to wounds, an effect that was abrogated in STAT3 knockdown wounds. These findings were supported in vitro. IL-10 promoted VEGF and CXCL12 synthesis in primary murine dermal fibroblasts, with blunted VEGF expression upon blocking CXCL12 in the media by antibody binding. IL-10-conditioned fibroblast media also significantly promoted endothelial sprouting and network formation. In conclusion, these studies demonstrate that overexpression of IL-10 in dermal wounds recruits EPCs and leads to increased vascular structures and faster re-epithelialization.

#### KEYWORDS

angiogenesis, diabetes, endothelial progenitor cells, IL-10, VEGF, wound healing

## 1 | INTRODUCTION

Chronic wounds are prevalent and particularly debilitating in diabetic patients. This is partly due to impaired neovascularization, which ultimately leads to recurrent infections, failure to heal, and extremity amputations, thus imposing substantial economic healthcare burdens.<sup>1–3</sup> In contrast, physiologic dermal wound healing in healthy individuals is characterized by a well-coordinated series of responses to injury, including granulation tissue formation, epithelial gap closure, inflammatory regulation, and robust neovascularization—a process initiated by local endothelial cells and by both circulating and tissue resident endothelial progenitor cells (EPCs)—to effectively restore circulation to the affected area and support tissue repair.<sup>4</sup>

Endothelial progenitor cells (EPCs) contribute to wound neovascularization<sup>5–7</sup> by differentiating and incorporating into de novo endothelial vascular structures,<sup>8,9</sup> and by paracrine effects via the production of growth factors that support vascularization.<sup>10,11</sup> EPCs can be broadly classified into early and late EPCs, and although their phenotype continues to evolve,<sup>12</sup> CD34, CD31/PECAM1, VEGFR2/Flk1/KDR, and CD133 are archetype cell markers to define these progenitor cells.<sup>13,14</sup> More importantly, and consistent with the relevance of EPC-driven neovascularization in tissue repair, impaired mobilization and recruitment of EPCs have been implicated in diabetic wounds.<sup>15–25</sup> Therefore, it is important to develop innovative strategies aimed at improving molecular signals that trigger EPC mobilization, homing, survival, and function as a means to ultimately

achieve a meaningful clinical impact in the treatment of chronic wounds.<sup>26–30</sup>

One of the factors that mobilize EPCs from the bone marrow (BM) into circulation after injury is vascular endothelial growth factor (VEGF),<sup>31–33</sup> which is produced in injured tissues in response to hypoxia.<sup>34</sup> VEGF is known to activate BM matrix metalloproteinase-9 (MMP-9), which in turn releases stem cell factor (SCF) to facilitate EPC proliferation and mobilization from the BM niche into the peripheral circulation.<sup>35</sup> Furthermore, recent studies have shown that VEGF promotes CXC motif chemokine 12 (CXCL12)-, formerly stromal cell-derived factor 1 alpha (SDF-1 $\alpha$ ), and CXC motif chemokine receptor 4 (CXCR4)-dependent signaling, leading to homing of bone marrow hematopoietic progenitor and stem cells and cardiac stem cells to tissue repair sites in models of myocardial infarction.<sup>36,37</sup> This signaling pathway is also known to be involved in EPC homing to sites of hypoxia/ischemia.<sup>38–42</sup> Previous studies demonstrated that fibroblasts are likely a critical source of VEGF and CXCL12 production in cutaneous wounds.<sup>43,44</sup> Existing evidence indicates that CXCL12 is constitutively expressed by BM stromal cells and in so doing plays a key role in maintaining the BM niche, as well as providing directional cues that orchestrate CD34<sup>+</sup> cell homing to injured tissues. Under homeostatic conditions, high CXCL12 expression in the BM is considered a strong chemotactic factor, whose function is to retain CD34<sup>+</sup> progenitor cells within the BM niche. After an injury, CXCL12 is released by the injured tissue,<sup>44,45</sup> and the higher local levels of CXCL12 stimulate mobilization of progenitor cells out from the bone

marrow and their recruitment to the injury site. Hattori et al. demonstrated that elevated CXCL12 levels in peripheral blood results in the mobilization of these cells to the peripheral circulation.<sup>42</sup> In support of this finding, it has been shown that EPCs can be recruited from the bone marrow into peripheral hypoxic/ischemic tissue sites in response to treatment with CXCL12 and/or VEGF.<sup>46</sup> However, the high concentrations and multiple doses needed for individual angiogenic growth factors to affect a relevant clinical outcome are problematic. In addition, the growth and chemotactic factors such as VEGF, granulocyte colony stimulating factor (G-CSF), SCF, and CXCL12 that have been used for EPC mobilization have also been shown to induce hematopoietic stem and progenitor cell, as well as monocyte and macrophage, mobilization; by increasing the inflammatory burden at the tissue repair site, this undue mobilization may have negative effects on wound repair and healing.<sup>47</sup> In other words, while it is plausible that angiogenic growth factor treatment improves progenitor cell homing and EPC-mediated vascular remodeling, it is equally conceivable that it may affect the survival and/or function of EPCs at the sites of tissue repair due to increased inflammation.

Notably, studies in a murine myocardial infarction model showed that IL-10, a potent anti-inflammatory cytokine,<sup>48,49</sup> facilitates EPC mobilization and revascularization.<sup>45</sup> Moreover, IL-10-transfected EPCs adoptively transferred into the retinal microenvironment of diabetic rats showed improved vascular repair.<sup>50</sup> Although these collective findings support the role of IL-10 in EPC-mediated neovascularization, the mechanisms that determine such a function in cutaneous wounds remain to be elucidated. We and others have shown that IL-10 overexpression in postnatal cutaneous dermal wounds induces regenerative (scarless) tissue repair via inflammatory regulation<sup>51–53</sup> and fibroblast-mediated formation of an extracellular wound matrix rich in hyaluronan<sup>54</sup> via STAT3-dependent signaling.<sup>55,56</sup> However, the ability of IL-10 to drive EPC recruitment and neovascularization, along with its potential to promote dermal wound re-epithelialization, has been largely unstudied.

We hypothesized that, upon injury to the skin, IL-10 stimulates the local expression of VEGF and CXCL12 to mobilize and recruit EPCs into cutaneous wounds in a STAT3-dependent manner, inducing neovascularization and promoting wound healing. To obtain experimental evidence that supports our hypothesis, we studied IL-10 overexpression in non-diabetic and diabetic murine models of dermal wound healing using a previously described lentivirus (LV) transduction approach.<sup>51,54</sup> To assess the proposed contribution of STAT3 signaling, we investigated

IL-10 mediated tissue repair using a recently developed skin-specific STAT3 knockdown mouse model.<sup>54</sup>

## 2 | MATERIALS AND METHODS

### 2.1 | Generation of inducible STAT-3 knockout transgenic murine model

All animal procedures were approved by Cincinnati Children's Hospital Medical Center and Baylor College of Medicine Institutional Animal Care and Use Committee. 8–12-week old wild type (WT) mice (C57BL/6J; hereafter referenced as WT), type II diabetic mice (BKS. Cg-m+/+Lepr<sup>db</sup>/J; hereafter referenced as db/db), MMP-9 knockout (KO) mice (FVB.Cg-Mmp9tm1Tvu/J) and strain-matched WT mice (FVB/NJ) were purchased from Jackson laboratories (Bar Harbor, ME). Db/db mice with serum glucose >400 mg/dl and weight >40 g were used in all experiments. Conditional STAT3 KO mice were developed as explained previously.<sup>54</sup> Briefly, B6.Cg-Tg(UBC-cre/ERT2)1Ejb/J Cre-expressing mice, driven by the human ubiquitin C (UBC) promoter, were bred to mice containing a loxP-flanked STAT3<sup>fllox/fllox</sup> sequence (Jackson Laboratories). Double transgenic phenotype (STAT3<sup>Δ/Δ</sup>) was confirmed by genotyping,<sup>54</sup> and 8–12-week old mice were used in all experiments. The dorsal skin was shaved, and 4-OHT was topically administered (10 mg/ml in sterile vegetable oil, 150  $\mu$ l every day for seven days) to activate Cre-mediated recombination and achieve STAT3 deletion (STAT3<sup>-/-</sup>) in the dorsal skin, with vegetable oil administration alone serving as vehicle control group (STAT3<sup>Δ/Δ</sup>ctrl). STAT3 knockdown in the skin was quantified using Western blotting and band densitometry on dorsal skin snips from treated area as described previously,<sup>54</sup> prior to using the mice in excisional wounding.

### 2.2 | Excisional wounding and tissue harvest

Mice were anesthetized with isoflurane inhalation (0.5 ml, titrated). Dorsal skin was shaved and prepared by scrubbing alternately with isopropyl alcohol and povidone-iodine. Mice were divided into two treatment groups, where the left side dorsal flank was pre-treated with either 50  $\mu$ l of  $1 \times 10^6$  TU/ml of lentiviral IL-10 +/- ires GFP or lentiviral control +/- GFP, injected intradermally and labeled with India ink ( $n = 4–6$  mice/treatment group at each time point; both male and female). PBS labeled with India ink was injected in the bilateral flank as an internal control. A third group of mice, where both the



bilateral flanks were pre-treated with intradermal injection of PBS labeled with India ink, served as the external control treatment group. After 4 days to allow transgene expression, mice were anesthetized and two full thickness excisional wounds extending to the panniculus carnosus were created on both flanks at the treatment sites using a 4 mm biopsy punch (Miltex, Plainsboro, NJ). To prevent skin contraction, 6 mm silicone stents were secured around the wounds with skin glue and 6–8 interrupted sutures with 6–0 nylon (Ethicon Inc., Somerville, NJ). Stented wounds were covered with Tegaderm™ (3 M, St. Paul, MN). In STAT3 mice cohorts, daily topical administration of 4-OHT or vegetable oil was continued. Specifically, in MMP9<sup>-/-</sup> mice, in order to rescue the deficiency in release of SCF caused by lack of MMP9 and to reinstate endothelial progenitor cell mobilization, 0.5 µg/kg of SCF (Peprotech, Rocky Hill, NJ) was injected daily post wounding via tail vein.<sup>47</sup>

At day three and day seven post-wounding, mice were euthanized and peripheral blood, wounded skin, and femur and iliac bones were collected. The bone marrow was flushed out with saline and stored at -80°C. Wounds were bisected, and one half was fixed in 10% formalin, and paraffin-embedded. The other half was processed for RNA and protein isolations.

### 2.3 | Histologic evaluation of wound morphology

5 µm wound sections were cut from paraffin blocks. Epithelial gap closure and granulation tissue deposition were analyzed via Hematoxylin and Eosin (H&E) staining and morphometric image analysis using Nikon Elements (Nikon Instruments, Melville, NY). Wound ECM composition was determined using Movat's Pentachrome staining as per the manufacturer's protocol (Polyscientific, Bay Shore, NY).

### 2.4 | Immunohistochemical staining

5 µm serial sections were dewaxed in three changes of xylene for 10 min each and rehydrated in an ethanol to distilled water series. Antigen retrieval was performed using 1× Target Retrieval Solution (Dako, Carpinteria, CA) at 95°C for 20 min followed by a cool down to room temperature. Following a five-minute wash in distilled water, sections were permeabilized in 1× Phosphate Buffered Saline with 0.1% Tween (PBSTw) for 10 min. Endogenous peroxidase was blocked with 3% H<sub>2</sub>O<sub>2</sub> followed by blocking of nonspecific protein binding with a solution of 5% Rabbit Serum +1% Bovine Serum Albumin in PBSTw

for 2 h at room temperature. A M.O.M kit (Vector Laboratories, Burlingame, CA) was applied to slides per manufacturer's instructions if mouse monoclonal primary antibodies were used. Immunostaining with antibodies against CD45 (1:2500, Abcam ab10558, Cambridge, MA), Lamp2a (1:50; Abcam ab18528), MECA-32 (1:10, deposited to the Developmental Studies Hybridoma Bank, University of Iowa by Butcher), STAT3 (1:500, Cell Signaling Technology 9139, Danvers, MA), Phospho-STAT3 (Tyr705) (1:200, Cell Signaling 9145), TGF-β1 (1:100, Abcam ab92486), and TGF-β3 (1:100, Abcam 15537) was performed for one hour at room temperature, followed by incubation with biotinylated species specific secondary antibodies (1:200, Vector Laboratories). ABC-DAB peroxidase-based staining followed by hematoxylin counter staining (Vector Laboratories) was performed, and slides were dehydrated and mounted in xylene based permanent mounting media.

Endothelial progenitor cells (EPCs) were identified using double immunofluorescent staining for CD133, and Flk-1. 5 µm paraffin sections were prepared similar to above and autofluorescence was blocked using 50 mM Ammonium Chloride for 20 min. Following a rinse in PBSTw, nonspecific protein binding was blocked with a solution of 5% Normal Goat Serum, 1% Bovine Serum Albumin in PBSTw for two hours at room temperature. Primary antibodies were labeled according to the Zenon Complex Formation protocol (Invitrogen, Carlsbad, CA). A 3:1 molar ratio of Fab to antibody target was used for CD133 (AbCam ab19898), and 6:1 molar ratio for FLK-1 (AbCam, ab2349). The CD133-488 complex was diluted 1:250, while the FLK-1-647 complex was diluted 1:25 in block and incubated for one hour at room temperature. The sections were then washed three times in PBSTw for 5 min. Following the washes, the antibody-Fab complex was fixed to the samples using 4% paraformaldehyde for 15 min. The samples were then washed three times in PBS and mounted using Prolong Gold plus DAPI (Invitrogen).

The average number of CD45+, Lamp2a+, and CD133+Flk-1+ cells was quantified by counting positive cells in six high power fields (HPF, 40×) per wound section. Capillary lumen density was measured as the average number of MECA32-positive lumens from six HPF (40×) per section. HPF were equally distributed between the two wound edges.

### 2.5 | Flow cytometry

350 µl of whole blood per mouse was collected. Red blood cells were lysed using lysis solution per manufacturer's instructions (Qiagen, Alameda, CA). The cells were washed and centrifuged twice in 10 ml of 1% BSA-PBS

and re-suspended in 1 ml of 1% BSA-PBS solution and counted. EPCs were co-labeled using APC-conjugated anti-CD34 (1  $\mu$ l per  $5 \times 10^6$  cells), FITC-conjugated anti-CD133 (1.5  $\mu$ l per  $1 \times 10^6$  cells), and PE-conjugated anti-Flk-1 (2  $\mu$ l per  $1 \times 10^6$  cells) monoclonal antibodies (BD Biosciences, San Jose, CA) in the dark for 20 min at 4°C with gentle rocking. Unstained control and individual color controls were also included for gating. Cells were washed and re-suspended in 350  $\mu$ l of medium containing 7-AAD viability stain for live/dead discrimination (3  $\mu$ l per  $1 \times 10^6$  cells, eBioscience, San Diego, CA). Using the FACS Canto-II flow cytometer (BD Biosciences, San Jose, CA), single cells were gated to obtain a live CD34-positive population. Within this population, cells that co-expressed CD133 and Flk-1 were counted as EPCs. Each data point included at least 1 000 000 events. Flow data were then analyzed using the FlowJo software (Tree Star Inc., Ashland, OR) by a blinded investigator.

## 2.6 | Primary cell culture experiments

Primary adult (8–10 week old) murine dermal fibroblasts were isolated from the skin of C57BL/6J mice (Jackson Laboratories, Bar Harbor, ME, USA) using standard isolation protocols.<sup>57</sup> The fibroblast culture was routinely maintained at 37°C under 5% CO<sub>2</sub> in a humidified chamber and cultured in Dulbecco's Modified Eagle's media (DMEM; GIBCO, Carlsbad, CA, USA) supplemented with 10% bovine growth serum (BGS; Hyclone, Logan, UT, USA), 100 U penicillin, 100  $\mu$ g streptomycin +0.25  $\mu$ g amphotericin B (PSF; Invitrogen, Carlsbad, CA, USA). All cells used were between passages 5–10.

Fibroblasts were seeded at  $2 \times 10^5$  cells/well in a six-well plate in DMEM containing 10% BGS and allowed to settle overnight. Cells were then serum starved in DMEM culture media with 2% BGS, and the conditioned culture was supplemented with 200 ng/ml of murine IL-10 recombinant protein (Peprotech, Rocky Hill, NJ). After 48 h, supernatant was collected to investigate the effect of IL-10 stimulation on VEGF and CXCL12 production by the fibroblasts. Cells from two different passages were tested in triplicate experiments.

## 2.7 | Aortic ring assay

An aortic ring assay was performed as described previously.<sup>58</sup> Briefly, thoracic aortas were dissected from 8 to 10 week old male and female C57BL/6J mice after euthanasia. The periaortic connective tissue was carefully removed under a dissecting scope (M80 Stereomicroscope, Leica Microsystems, Buffalo Grove, IL) without damaging

the vessel wall. The aorta was then cut into 0.5 mm wide rings using a #10 blade and affixed on a culture dish with a thin layer of growth factor-reduced basement membrane matrix Matrigel (Corning, NY) and covered with DMEM culture media. These rings were first serum-starved overnight in DMEM containing no serum to equilibrate their growth factor responses. Aortas were grown in (1) DMEM complete media similar to the primary culture described earlier, (2) DMEM complete media supplemented with 200 ng/ml of murine IL-10 recombinant protein, (3) conditioned media from untreated adult dermal fibroblasts, or (4) conditioned media from adult dermal fibroblasts treated with 200 ng/ml of murine IL-10 recombinant protein. Conditioned media for conditions 3 and 4 was from primary cell culture experiments used for detection of growth factor production as described above. Three rings per treatment were studied, and the experiment was repeated two times with aortas from different mice and conditioned media from different primary cell isolations. The media was changed every 2–3 days. Sprout outgrowth was monitored on alternate days using phase contrast imaging (Leica DMI8). The image analysis software LASX (Leica) was used to measure the relative sprouting area (calculated as the difference in ring area between days 1 and 12).

## 2.8 | Quantitative real-time PCR

Wound tissue was homogenized in RLT buffer, and total RNA was isolated per manufacturer's recommendations (mini kit, Qiagen, Valencia, CA, USA). cDNA was synthesized from 1  $\mu$ g of RNA using the High Capacity cDNA Reverse Transcription kit (Applied Biosystems, Foster City, CA, USA) following manufacturer's protocols. SYBR green assays were designed to span intron/exon boundaries. Oligonucleotides were aligned against the mouse genome by Primer-BLAST ([www.NCBI.org](http://www.NCBI.org)) to ensure specificity. Gene expression was assayed in triplicate using 1/40th of the cDNA template, and 300 nM of forward and reverse primer in a 25  $\mu$ l Power SYBR Green PCR Master Mix reaction in the StepOne-Plus Real-Time PCR System (Applied Biosystems). Gene expression was normalized to mouse RPS29 gene expression. Relative expression values were calculated using the Comparative Ct ( $\Delta\Delta C_t$ ) method.<sup>59</sup> Oligonucleotide primer sequences used were as follows:

VEGFa 1F 5'-TTAAACGAACGTACTTGCAGATG-3' and 1R 5'-AGAGGTCTGGTTCCCGAA-3'.

CXCL12 1F 5'-GGTCTTCGAGAGCCACATCG-3' and 1R 5'-ACGGATGTCAGCCTTCCTCG-3'.

Rps29 1F 5'-TCTGAAGGCAAGATGGGTAC-3' and 1R 5'-GTGGCGGTTGGAGCAGACG-3'.

## 2.9 | Enzyme-linked immunosorbent assays

Wound tissue was homogenized in 50 mM Tris-HCl buffer containing 1% NP40, aprotinin (3.3 µg/ml), leupeptin (10 µg/ml), and pepstatin (4 µg/ml) and stored at  $-80^{\circ}\text{C}$  until testing (Sigma-Aldrich, St. Louis, MO). VEGF and CXCL12 protein levels were determined using Quantikine Enzyme-linked immunosorbent assays (ELISA) Kits (R&D Systems, Minneapolis, MN) per manufacturer's instructions. ELISA data were normalized to total protein in each sample, protein calculated using the Coomassie Plus protein assay (Thermo Scientific, Logan, UT).

## 2.10 | Statistical analyses

Data were analyzed using ANOVA followed by Tukey post-hoc means comparison test. The data are expressed as mean  $\pm$  standard deviation. Differences at  $p < .05$  were considered to denote statistical significance.

## 3 | RESULTS

### 3.1 | IL-10 overexpression improved wound re-epithelialization and reduced inflammatory cell infiltration via a STAT3-dependent mechanism

We sought to determine the effect of IL-10 overexpression on the early wound healing responses, including wound re-epithelialization, granulation tissue formation, and neovascularization, which have not been previously studied. To further determine whether these effects of IL-10 were mediated via conserved STAT3 signaling, we used a tamoxifen (4-OHT)-inducible cre driven skin-specific STAT3 knockout murine model. We generated the STAT3 $\Delta/\Delta$  transgenic mice as described previously.<sup>54</sup> Topical application of 4-OHT in vegetable oil as a vehicle down-regulated STAT3 levels in the skin of these mice, compared to topical application of vegetable oil vehicle alone, which served as vehicle control for all experimental purposes (Figure S1).

Prior to assessing the effect of IL-10 overexpression on wound healing, we first compared baseline wound healing with PBS (moist wound) control treatment in the three groups of mice, i.e., C57BL/6J (WT), STAT3 $\Delta/\Delta$  Ctrl, and STAT3 $^{-/-}$ , and showed that at day three, epithelial gap closure and granulation tissue formation in STAT3 $\Delta/\Delta$  Ctrl transgenic mice was comparable to WT mice. Further, these parameters were not affected in STAT3 $^{-/-}$  mice wounds (Figure 1G,H; dotted line represents PBS wounds

in WT). These data confirm that the ~60% STAT3 knock-down we achieved at the protein levels in the skin of 4-OHT-treated transgenic mice has no impact on the baseline ability of these mice to heal cutaneous wounds.

Next, we evaluated the effect of lentiviral-transduced IL-10 (LV IL-10) overexpression on wound healing at day 3 post wounding. Similar to our previous reports, where we demonstrated efficient transduction with transgenic protein expression detected at the base of wounds within 72 h of treatment, we saw a significant increase in IL-10 levels at day 3 post-wounding as well as enhanced phosphorylated-STAT3 signaling in STAT3 $\Delta/\Delta$  Ctrl transgenic mice wounds treated with LV IL-10 (Figure S2). Histologic observation and morphometric analysis of day 3 wounds in STAT3 $\Delta/\Delta$  Ctrl mice demonstrated that IL-10 overexpression significantly enhanced the speed of epithelial gap closure and was associated with robust granulation tissue formation. LV GFP and PBS control wounds, in comparison, had a paucity in granulation tissue and reduced travel distance of the encroaching epithelial margins (Figure 1A–C,G,H, arrow heads indicate edge of the punch wound, arrows indicate the tip of the encroaching epithelial tongues). As expected, the effects of IL-10 were abrogated in STAT3 $^{-/-}$  mice (Figure 1F), which had comparatively similar epithelial gap closure and granulation tissue formation to that observed in LV GFP or PBS wounds (Figure 1D–H), providing support for the postulate that IL-10's effects are mediated via downstream STAT3 signaling.

At day 7 the extent of epithelial gap closure was similar between PBS-, LV GFP-, and LV IL-10-treated STAT3 $\Delta/\Delta$  Ctrl mice (Figure 2A–C). However, at the same time point, IL-10-treated wounds demonstrated more organized cell layers in the epidermis, and robust granulation tissue (Figure 2G), with uniform distribution of the cellular density throughout the healing wound. Moreover, wounds treated with LV IL-10 had a greater degree of collagen deposition in the wound center (Figure S3). In contrast, LV GFP- (Figure 2B,E) and PBS-treated (Figure 2A,D) wounds demonstrated dense cellularity only at the encroaching edges, with lower cell density and collagen staining at the wound center, indicating a slower progress of wound healing. As anticipated, LV IL-10 treatment also significantly decreased the CD45 $^{+}$  (Figure 2H) and Lamp2a $^{+}$  (Figure 2I) inflammatory cell burden in the wound compared to LV GFP and PBS controls. Similarly, immunohistochemical evaluation of TGF- $\beta$ 1 and - $\beta$ 3 staining showed that LV IL-10-treated wounds had comparable TGF- $\beta$ 1 wound bed expression patterns to those of control wounds (Figure 2J), but higher TGF- $\beta$ 3 wound bed expression (Figure 2K). Conversely, the previously-seen effect of IL-10 on granulation tissue formation (Figure 2D–G), inflammatory cell infiltration (Figure 2H,I) and TGF- $\beta$ 3



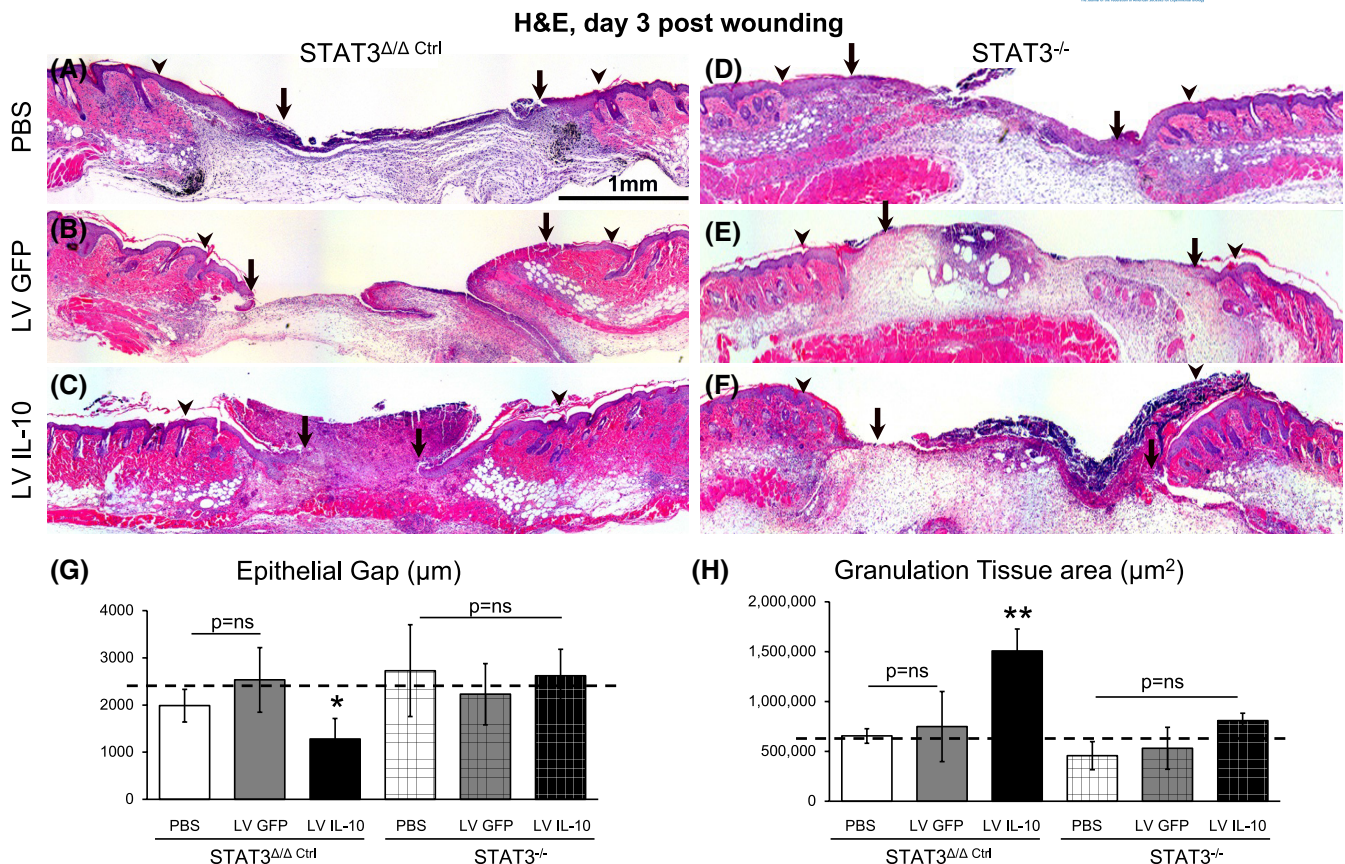


**FIGURE 1** IL-10 overexpression enhanced wound closure in a STAT3-dependent manner in vivo. (A–F) Hematoxylin and Eosin staining of wounds at day 3 post wounding. Wounds are marked in India ink; wound margins are indicated by arrowheads and the encroaching epithelial margins are indicated by arrows. (A–F) Original magnification: 4 $\times$ , Scale Bar = 500  $\mu\text{m}$ ; As compared to PBS (A) or lentiviral GFP (B) control treatments, lentiviral IL-10-treated wounds show enhanced wound closure and robust granulation tissue formation (C) in STAT3 $\Delta/\Delta$  ctrl vehicle control mice. IL-10's effects on wound healing were abrogated in STAT3 $^{-/-}$  mice, as evidenced by significantly impaired wound morphology (D–F). (G and H) Quantitation of epithelial gap (G) and granulation tissue (H) amongst the different treatments based on image analysis show that while there is no significant difference in gap closure between PBS and lentiviral GFP wounds, lentiviral IL-10 treated wounds exhibit increased gap closure and granulation tissue formation, whereas in STAT3 $^{-/-}$  mice this effect is abrogated. Bar plots: mean  $\pm$  SD, 2 sections/wound,  $n = 4$  wounds from different mice/treatment group, \*\*\* $p < .001$  by ANOVA

expression (Figure 2K) was largely abrogated in STAT3 $^{-/-}$  mice and resulted in a wound healing response similar to LV GFP and PBS control wounds. Taken together, these data support our prediction that IL-10 overexpression improves initial wound re-epithelialization and granulation tissue deposition at day 3 and 7 by mechanisms that are STAT3-dependent, ultimately leading to superior remodeling and regeneration phenotype at 1 month post wounding that we have recently reported.<sup>54</sup>

### 3.2 | IL-10 overexpression increased capillary density and EPC infiltration of the wound tissue via STAT3

We then investigated the effect of IL-10 overexpression on wound capillary density and EPC infiltration. To that end, we performed immunohistochemical staining with

MECA-32, a pan-endothelial cell antigen: LV IL-10-treated wounds in STAT3 $\Delta/\Delta$  ctrl mice developed vessels with well-defined lumens at day 7, in contrast to control LV GFP- or PBS-treated wounds, which showed mostly non-cohesive individual cell staining (Figure 3A–C). LV IL-10-treated wounds also showed significantly increased capillary lumen density per high power field (LV IL-10:  $24.17 \pm 2.69$  vessels/HPF vs. LV GFP:  $15.7 \pm 2.49$ , PBS:  $14.6 \pm 3.8$ ,  $p < .001$ ; Figure 3M). In contrast, STAT3 $^{-/-}$  wounds treated with LV IL-10 failed to achieve the anticipated effects on capillary lumen density (STAT3 $^{-/-}$  + LV IL-10:  $12.18 \pm 4.18$  vessels/HPF vs. STAT3 $\Delta/\Delta$  ctrl + LV IL-10:  $24.17 \pm 2.69$ ,  $p < .001$ ; Figure 3D–F,M).

Similarly, LV IL-10-treated wounds in STAT3 $\Delta/\Delta$  ctrl mice had significantly increased infiltration of CD133 $^{+}$ /Flk-1 $^{+}$  EPCs, as shown by immunofluorescence co-labeling at day 7 after wounding (LV IL-10:  $5.17 \pm 1.03$  EPCs/HPF vs. LV GFP:  $2.43 \pm 0.97$ , PBS:  $3.13 \pm 1.42$ ,  $p$

< .01; Figure 3G–I,N). In contrast, LV IL-10 once again failed to achieve the anticipated increase in wound EPC expression when administered to STAT3<sup>-/-</sup> mice, wherein the EPC count was no different than that quantified in LV GFP- or PBS-treated control wounds (STAT3<sup>-/-</sup> + LV IL-10:  $3.38 \pm 1.63$  EPCs/HPF vs. STAT3<sup>Δ/Δ</sup> ctrl + LV IL-10:  $5.17 \pm 1.03$ ,  $p < .01$ ; Figure 3J–L,N). These data further support the significant role of IL-10 in driving both vascular structures and EPC recruitment to wounds as part of its function in regulating cutaneous wound healing and underscore the dependence of this process on STAT3 signaling.

### 3.3 | IL-10 overexpression increased EPC mobilization in response to wounding via a STAT3-dependent mechanism

We then determined whether the increase in EPC counts in LV IL-10-treated wounds was facilitated by an increase in EPC mobilization. As we have previously shown that in response to cutaneous wounding, EPC levels peak in peripheral blood at day 3 post-injury,<sup>60</sup> we evaluated the peripheral blood for the presence of CD34<sup>+</sup>CD133<sup>+</sup>Flk-1<sup>+</sup> co-labelled cells in STAT3<sup>Δ/Δ</sup> ctrl and STAT3<sup>-/-</sup> mice after treatment of their cutaneous wound with LV IL-10, LV GFP and PBS using flow cytometry (Figure 4A–C).

Similar to our previous study,<sup>60</sup> our data shows that in comparison to unwounded mice, skin wounding and moist treatment with PBS alone resulted in a significant ( $p < .01$ ) increase in circulating levels of EPCs at day 3 post-wounding in STAT3<sup>Δ/Δ</sup> ctrl mice (Figure 4B–D:  $3.54 \pm 0.85$  vs.  $7.96 \pm 1.68$ ;  $p < .01$ ). However, LV IL-10 overexpression in STAT3<sup>Δ/Δ</sup> ctrl mice significantly increased the percentage of circulating EPC levels at day 3 post-wounding over that of mice treated with LV GFP or PBS controls (LV IL-10:  $24.58 \pm 6.35$  vs. LV GFP:  $9.28 \pm 3.0$ ,

PBS:  $7.96 \pm 1.68$ ,  $p < .01$ ; Figure 4D). Consistent with the other observations, LV-mediated IL-10 overexpression in STAT3<sup>-/-</sup> mice wounds did not experience this increase in circulating EPCs; EPC levels in these mice were analogous to LV GFP or PBS controls (STAT3<sup>-/-</sup> + LV IL-10:  $7.22 \pm 2.51$  vs. STAT3<sup>Δ/Δ</sup> ctrl + LV IL-10:  $24.58 \pm 6.35$ ,  $p < .01$ ; Figure 4D). These data show that IL-10 increased injury-induced mobilization of EPCs beyond physiologic levels and further uphold that the function of IL-10 overexpression in the cutaneous wound healing is STAT3-dependent.

### 3.4 | IL-10 increased VEGF expression via a STAT3-dependent mechanism

To investigate if IL-10-STAT3 signaling influences the expression of VEGF, a known promoter of EPC mobilization, we measured the levels of the growth factor under experimental conditions similar to those preceding. We specifically analyzed VEGF expression in the wound specimen, serum, and bone marrow (BM), as these tissue compartments represent the major microenvironments where VEGF-mediated signaling is known to facilitate injury-induced EPC mobilization. We found that, in comparison to unwounded mice, skin wounding and treatment with PBS moist treatment control significantly increased VEGF levels in all three of these compartments, most strongly in the wound itself as compared to expression levels in uninjured skin (Figure 5A–C). LV IL-10 treatment of wounds in STAT3<sup>Δ/Δ</sup> ctrl mice resulted in a further increase in VEGF levels in these three sites; while this increase trended but did not reach significance in wounded skin (Figure 5A;  $p = .64$ ), it was significant in serum (Figure 5B;  $p < .01$ ) and BM (Figure 5C;  $p < .05$ ). Once again, LV-mediated overexpression of IL-10 in STAT3<sup>-/-</sup> mice did not result in increased VEGF expression. To isolate which compartment of the wound contributed to expression of VEGF,

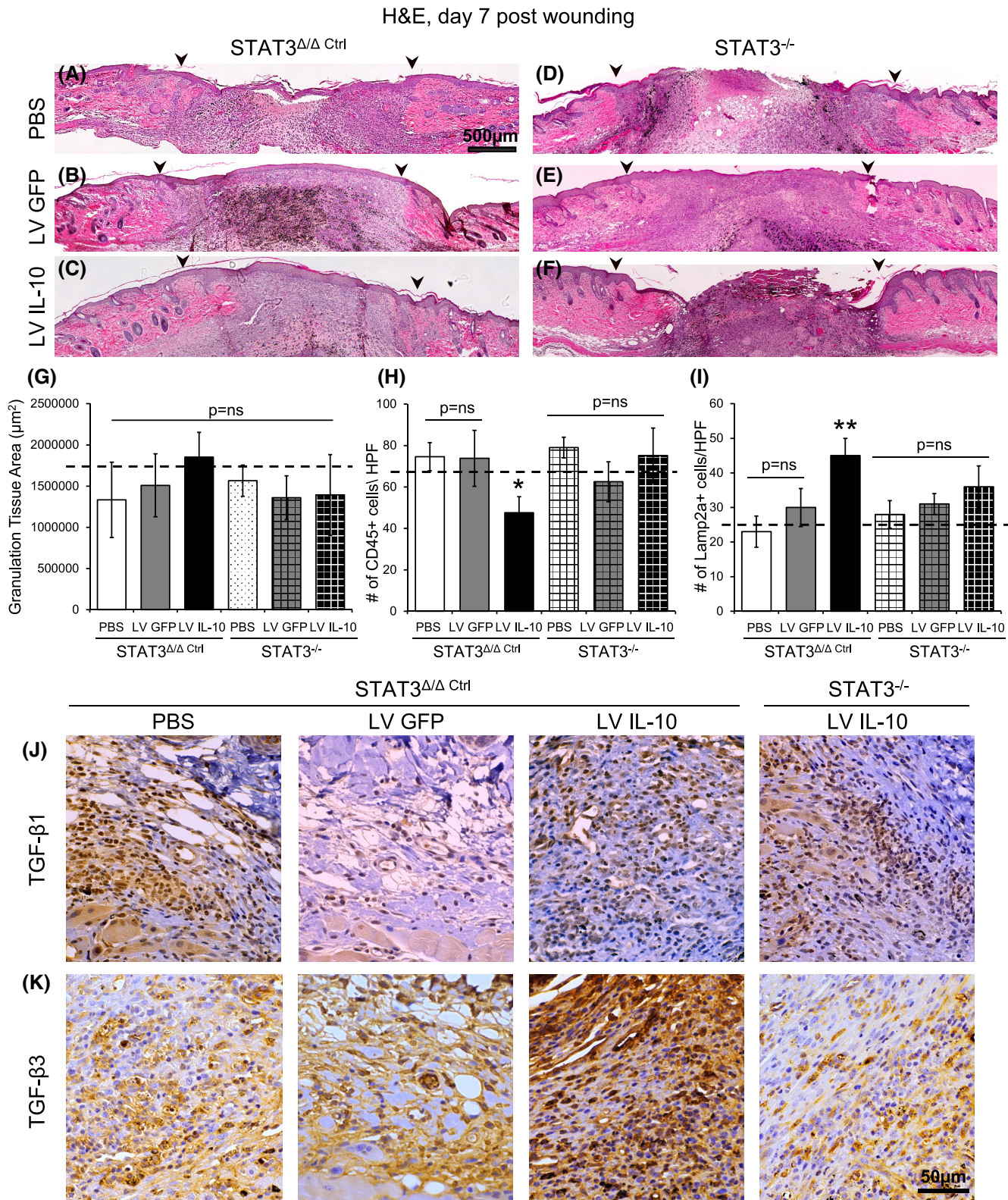
**FIGURE 2** IL-10 overexpression reduced inflammation and enhanced wound remodeling and regenerative phenotype in a STAT3-dependent manner. (A–F) Hematoxylin and Eosin staining of wounds at day 7 post wounding. Wounds are marked in India ink; wound margins are indicated by arrowheads. (A–F) Original magnification: 4×, Scale Bar = 500 μm; (A–C) similar gap closure is observed between the three groups—PBS, lentiviral GFP and lentiviral IL-10 treated wounds in STAT3<sup>Δ/Δ</sup> ctrl mice. However, IL-10 treated cohort display thicker epidermis and robust granulation tissue as compared to the control treatments. (D–F) All treatment cohorts healed similarly in STAT3<sup>-/-</sup> mice and the effect of IL-10 on the epidermis and granulation tissue deposition is not apparent. (F) Quantitation of granulation tissue between different treatment groups in STAT3<sup>Δ/Δ</sup> ctrl show a modest trend in IL-10 treated mice, however, with no statistical significance between STAT3<sup>Δ/Δ</sup> ctrl and STAT3<sup>-/-</sup> with different treatments. (H) quantification of staining with CD45 show significantly lower CD45+ cells per high power field (HPF; 40×) in lentiviral IL-10 wounds as compared to lentiviral GFP or PBS treatments in STAT3<sup>Δ/Δ</sup> ctrl mice, which is abrogated in STAT3<sup>-/-</sup> mice. (I) Elevated expression of Lamp2a positive cells was observed in lentiviral IL-10 treated wounds as compared to the control treatments in STAT3<sup>Δ/Δ</sup> ctrl mice, which is abrogated in STAT3<sup>-/-</sup> mice. (J) Panels left to right show similar TGF-β1 staining pattern in controls versus lentiviral IL-10 treated wounds in STAT3<sup>Δ/Δ</sup> ctrl mice, that remain similar in expression in STAT3<sup>-/-</sup> wounds. (K) A definite increase in TGF-β3 expression is seen in lentiviral IL-10 treated wounds as compared to control treated ones in STAT3<sup>Δ/Δ</sup> ctrl mice, however, this effect induced by IL-10 waned in STAT3<sup>-/-</sup> wounds. Scale bar = 50 μm in (J and K); Bar plots: mean ± SD, 2 sections/wound,  $n = 4$  wounds from different mice/treatment group, \*\*\* $p < .001$  by ANOVA



IHC staining was performed demonstrating greatest staining at the margins of the granulating wound bed in the dermis (Figure S5).

We sought to briefly explain how LV IL-10-induced VEGF overexpression in our model might be a major contributor to increase in EPC mobilization, using a

well-defined mouse model of MMP9 deficiency known to have impaired EPC mobilization after cutaneous wounding.<sup>47</sup> As VEGF-induced activation of MMP9 is essential for the release of SCF and thereby EPC mobilization from the BM niche into peripheral circulation,<sup>35</sup> an absence of functional MMP9 in this mouse model results in





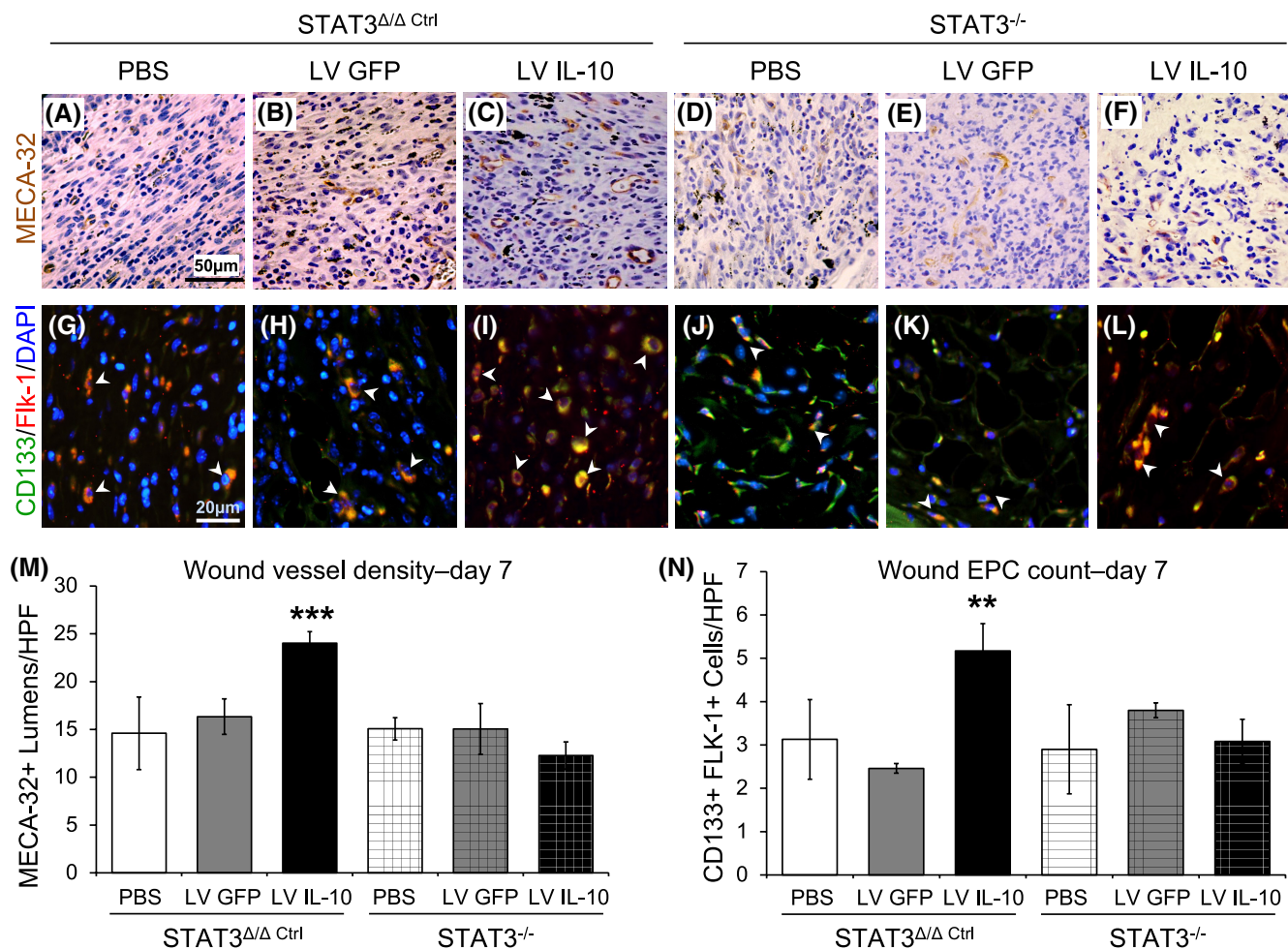


**FIGURE 3** IL-10 overexpression enhanced wound capillary lumen density and EPC infiltration in a STAT3-dependent manner. (A–F) Capillary lumens are marked by MECA-32 staining. (G–L) EPCs are identified by their characteristic morphology, large eccentric nuclei and CD133+/FLK-1+ staining (CD133–green, FLK-1–red, merged–yellow). Representative MECA-32+ and CD133+/FLK-1+ wound images for each treatment group at day 7 are shown here. Lentiviral IL-10 treatment significantly enhanced wound vessel density (*m*) and EPC numbers (*n*) per high power field (HPF), compared to lentiviral GFP or PBS treatments in STAT3 $\Delta/\Delta$  Ctrl mice, which was abrogated in STAT3 $^{-/-}$  mice. CD133+/FLK-1+ EPCs are indicated by arrow heads. Bar plots: mean  $\pm$  SD. 2 sections/wound, *n* = 3–4 wounds from different mice/treatment group, \*\*\**p* < .001 by ANOVA. Scale Bars = 50  $\mu$ m and Original magnification: 40 $\times$  in (A–F); Scale Bars = 20  $\mu$ m and Original magnification: 80 $\times$  in (G–L)

impaired EPC mobilization after cutaneous wounding. To investigate the role of VEGF/MMP9-mediated signaling in IL-10-dependent EPC mobilization, we created wounds in MMP9 $^{-/-}$  mice under similar experimental conditions as above. Consistent with previously reported findings, wounded MMP9 $^{-/-}$  mice had no change in levels of circulating EPCs at day 3 post-injury, proof of an impaired wound healing phenotype as compared to WT. As expected, and as shown previously by our group, administration of SCF to MMP9 $^{-/-}$  wounded mice reinstated EPC numbers in circulation. However, when LV IL-10 was overexpressed in MMP9 $^{-/-}$  mice wounds, VEGF levels increased in the serum, but did not restore EPC mobilization (Figure S4). These data suggest that, while LV IL-10 overexpression in the wound has a systemic effect on VEGF,

intact MMP9 function is likely also essential to the downstream signaling for IL-10 induced EPC mobilization.

### 3.5 | IL-10 treatment resulted in a positive CXCL12 concentration gradient via a STAT3-dependent mechanism

To investigate whether the effect of IL-10 on increasing circulating EPC levels and EPC presence in dermal wounds is mediated by CXCL12, we assessed levels of this chemotactic factor in wounds, serum, and BM at day 3 post-wounding. There was an increase in CXCL12 expression in wounded skin specimen (Figure 5D; *p* < .05) at day 3 post-injury when compared to expression levels

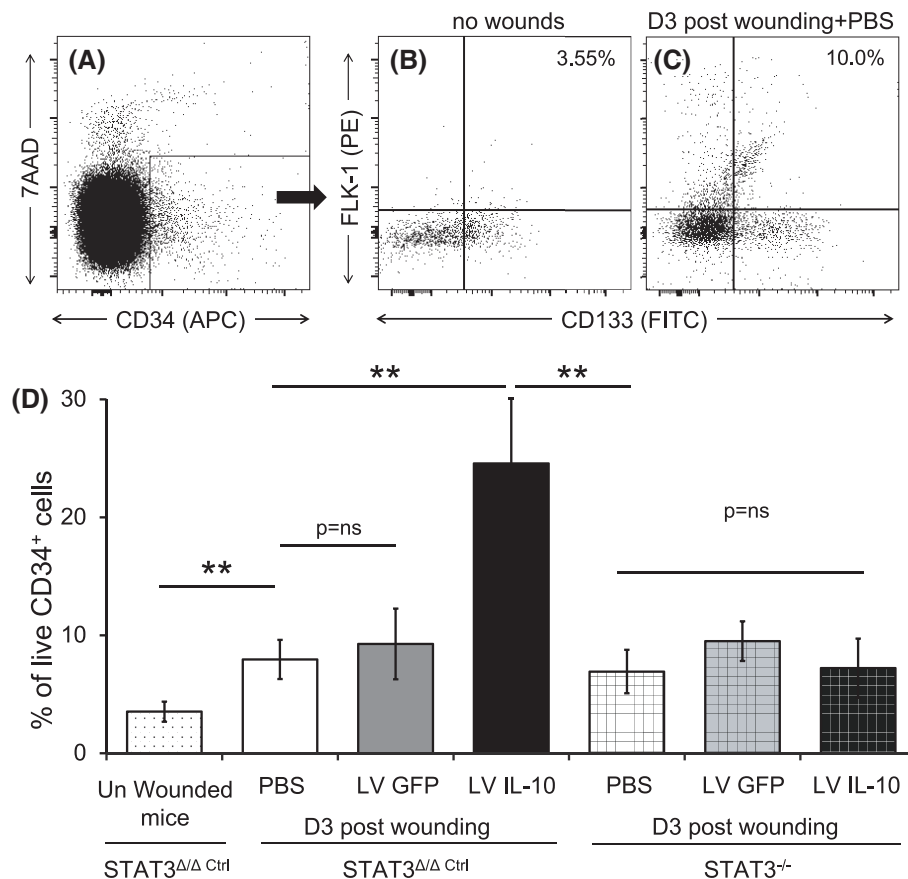


**FIGURE 4** IL-10 overexpression enhanced STAT3-dependent EPC mobilization after cutaneous wounding. Peripheral blood was collected at baseline before wounding and again at day 3 post wounding from STAT3<sup>Δ/Δ</sup> ctrl and STAT3<sup>-/-</sup> mice that received lentiviral IL-10, lentiviral GFP or PBS treatments. Cells were stained with 7AAD, CD34, CD133 and Flk-1 for flow cytometry analysis. (A) Single cells were gated for 7AAD<sup>-</sup> CD34<sup>+</sup> populations; of which cells that were CD133<sup>+</sup>Flk-1<sup>+</sup> were quantified as EPCs (B). There is a clear difference in EPC levels in peripheral blood at baseline in uninjured mice (B) versus mice at day three post wounding (C). (D) Quantitative analysis show that following cutaneous wounding there is a significant increase in EPCs at day 3 post wounding as compared to uninjured control mice. Lentiviral IL-10 treatment significantly increase circulating EPC levels as compared to lentiviral GFP or PBS treatments in STAT3<sup>Δ/Δ</sup> ctrl mice. IL-10's effects were abrogated in STAT3<sup>-/-</sup> mice. Bar plots = mean  $\pm$  SD of EPC numbers as analyzed by the FlowJo software,  $n = 3-4$  wounds from different mice/treatment group, \*\* $p < .01$  by ANOVA

in uninjured skin. No change in serum levels of CXCL12 was seen (Figure 5E), but a significant decrease in BM CXCL12 levels (Figure 5F;  $p < .01$ ) was noted in response to cutaneous wounding. These findings support the role of CXCL12 in the retention of EPCs in a quiescent niche under homeostatic conditions, and suggest that a positive CXCL12 gradient is established following wounding, which may facilitate the egress of EPCs from the bone marrow to the circulation and homing to the site of the wound. We also observed that LV IL-10 overexpression in the wounds of STAT3<sup>Δ/Δ</sup> ctrl mice at day 3 post-wounding resulted in significant increases in CXCL12 levels in wounded tissue (Figure 5D;  $p < .05$ ) and in the serum (Figure 5E;  $p < .001$ ) without affecting BM CXCL12 levels, as compared to LV GFP and PBS treatments (Figure 5F). LV IL-10's effect in increasing CXCL12 levels in skin wounds and serum, however, was consistently abrogated in STAT3<sup>-/-</sup> mice.

Immunohistochemical staining for CXCL12 in day 3 skin wounds demonstrated that majority of the positive cells are indeed present in the dermis (Figure S5). In addition, quantification of gene expression of CXCR4, a cognate receptor of CXCL12, in day 3 wounds showed upregulated expression in LV IL-10 wounds as compared to control-treated wounds (Figure S6). Collectively, these data indicate that IL-10 overexpression in skin wounds further promotes the wound-induced CXCL12 chemotactic gradient in a STAT3-dependent manner.

### 3.6 | IL-10 induced VEGF and CXCL12 production by fibroblasts

Because fibroblasts are important effector cells in wound healing and neovascularization, we investigated whether

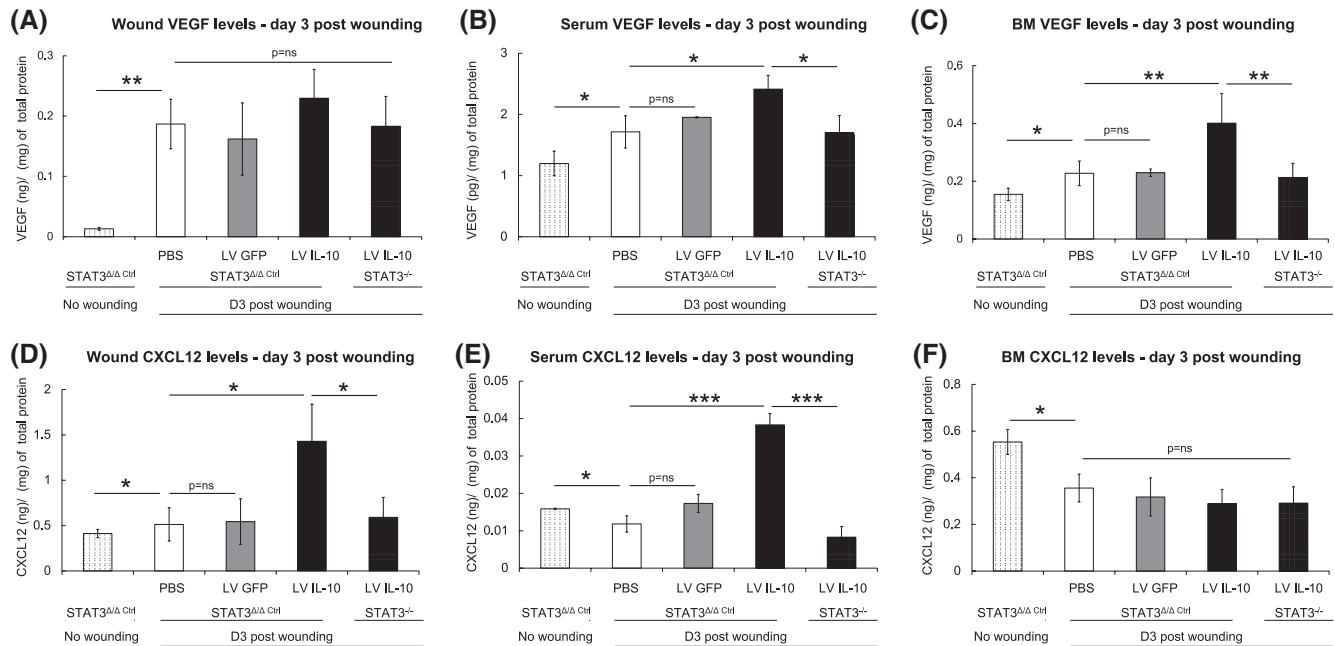


**FIGURE 5** IL-10 regulates VEGF and CXCL12 gradients in wounds, serum, and bone marrow in a STAT3-dependent manner.

Wound tissue, peripheral blood, and bone marrow (BM) were collected at baseline before wounding and again at day 3 post wounding from STAT3 $\Delta/\Delta$  Ctrl and STAT3 $^{-/-}$  mice that received lentiviral IL-10, lentiviral GFP, or PBS treatments. VEGF and CXCL12 levels were quantified with ELISA. The effect of different treatments on VEGF and CXCL12 levels within the wound tissue specimens, serum, and BM are respectively shown in (A–C) and (D–F). Bar plots = mean  $\pm$  SD,  $n$  = 3–4 wounds from different animals/treatment group, \* $p$  < .05, \*\* $p$  < .01, \*\*\* $p$  < .001 by ANOVA

fibroblasts are a potential source of IL-10-induced VEGF and CXCL12 expression. Consistent with this, we found that treatment with IL-10 significantly increased CXCL12 production in primary murine dermal fibroblasts in vitro (Figure 6A;  $p$  < .05). Furthermore, the same in vitro treatment of primary murine dermal fibroblasts with IL-10 also resulted in significantly increased VEGF levels (Figure 6B;  $p$  < .05). To determine if this IL-10 induced rise in VEGF is due to autocrine CXCL12 signaling, CXCL12 was inhibited using anti-CXCL12 mAb. This resulted in blunted VEGF production in AFB treated with IL-10 compared to AFB alone, suggesting there is indeed autocrine CXCL12 signaling in AFB that regulates VEGF secretion in response to IL-10. Together, these data provide evidence of the ability of fibroblasts to upregulate VEGF and CXCL12 levels in response to IL-10, and possibly of a central cellular role in the neovascularization process observed in our in vivo studies.

### 3.7 | Relative sprouting area and lumen density on aortic ring assay is increased in IL-10-treated fibroblast-conditioned media

The aortic ring assay is a simple but informative assay to identify modulators of angiogenesis by recapitulating the essential steps of microvessel outgrowth in vitro,

including proliferation, migration, tubule formation, and recruitment of supporting cells. We performed this assay by comparing aortic rings cultured in DMEM complete media spiked with IL-10 versus DMEM complete media alone to determine the effect of IL-10 on capillary outgrowth (Figure 6C–G). As anticipated from previous studies, aortic rings exposed to DMEM showed a robust endothelial cell (EC) outgrowth with a characteristic cobble stone-like appearance and a relative sprouting area (RSA) of  $4.86 \pm 0.37$  mm<sup>2</sup> at 12 days in culture (Figure 6C). Rings exposed to IL-10-spiked DMEM, however, had an RSA ( $3.21 \pm 1.5$  mm<sup>2</sup>) and also showed ECs organized into 2D networks (Figure 6D; arrowheads). We then repeated the aortic ring assays with conditioned DMEM supernatant from in vitro cultures of untreated adult dermal fibroblasts (AFB) versus conditioned supernatant from adult dermal fibroblasts treated with IL-10. When conditioned supernatant from untreated AFB was transferred, the aortic rings showed no measurable endothelial sprouting at day 12 (Figure 6E), suggesting that factors produced by normal fibroblasts under normal cell culture conditions perhaps support vessel stabilization, as opposed to sprouting. Aortic rings exposed to conditioned supernatant from AFB cultured in DMEM + IL-10 produced sprouting with an RSA of  $3.74$  mm<sup>2</sup>  $\pm$   $1.1$  mm<sup>2</sup>, but interestingly, this treatment resulted in a dense capillary-like network formation

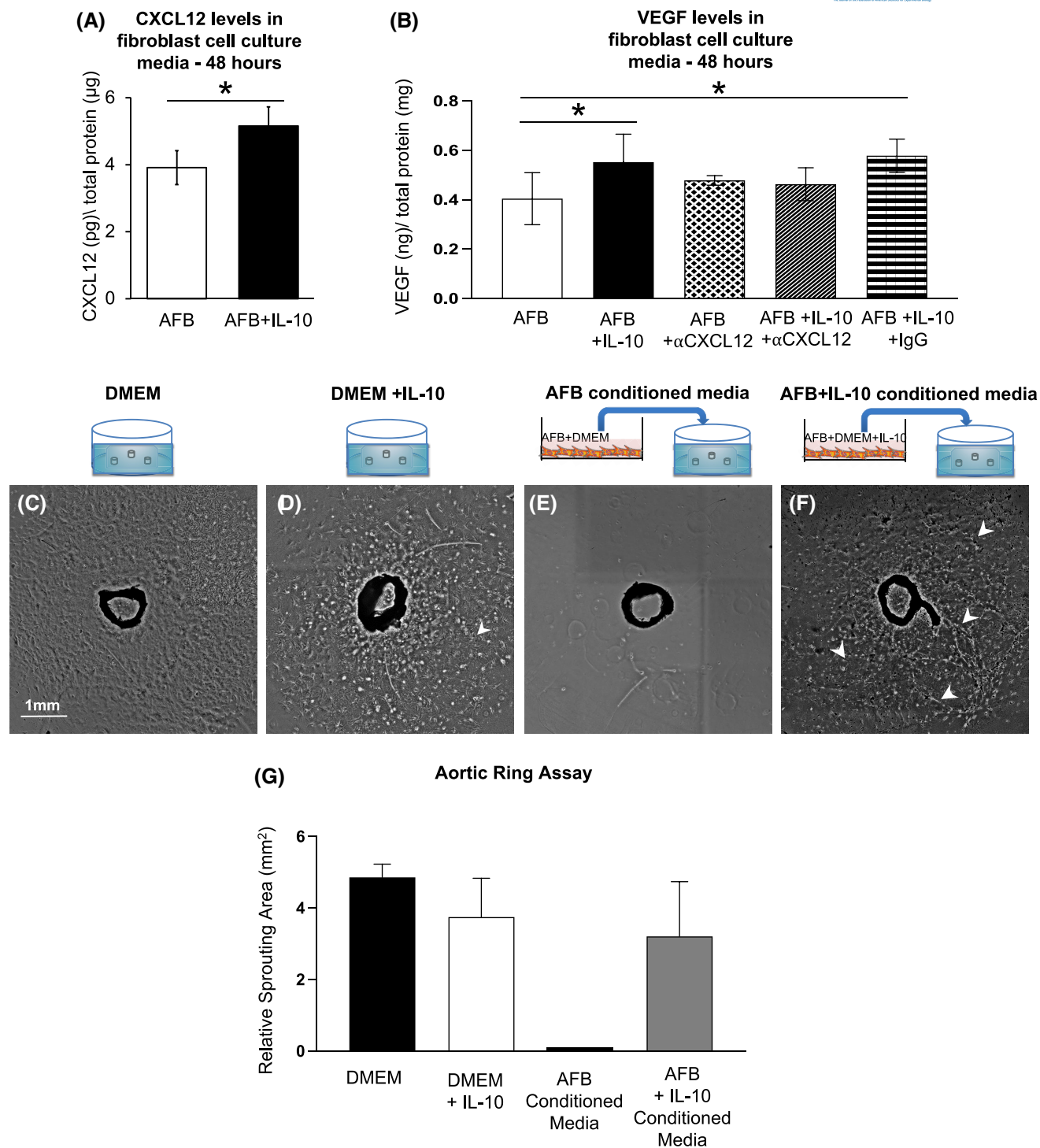


**FIGURE 6** IL10 induced VEGF and CXCL12 production in primary murine dermal fibroblasts and increased cell sprouting and capillary-like network formation in aortic ring assay. Primary murine dermal fibroblasts in culture were incubated  $\pm$  200 ng/ml of IL-10 for 48 h. Supernatants from the cultures were assayed for VEGF and CXCL12 expression by ELISA. (A) CXCL12 levels significantly increase in IL 10 treated fibroblasts as compared to untreated cells. (B) VEGF levels significantly increase in IL-10 treated fibroblasts as compared to controls, however not when anti-CXCL12 mAb is included in treatment. (C and D) Murine thoracic aortas are treated with either DMEM or DMEM supplemented with 200 ng/ml IL-10 for 12 days. Aortic rings show an endothelial cell outgrowth when treated with DMEM (C), and the ones spiked with DMEM + IL10 respond but with a similar relative sprouting area (D). (E and F) The aortic ring assay was repeated with either conditioned media from primary murine dermal fibroblasts, or conditioned media from fibroblasts treated with IL-10 from panel (A). The former produced no measurable endothelial outgrowth (E), whereas with the latter, a significant outgrowth with an increase in capillary-like 2D network formation was observed. Relative sprouting area for treatment groups quantified in (G). White arrowheads indicate the capillary-like networks. Bar plots: mean  $\pm$  SD, experiments are conducted in triplicates with cells from 2 passages; \* $p < .05$ , by ANOVA.  $n = 3$  aortic rings per treatment were studied and the experiment was repeated two times with aortas from different mice and conditioned media from different primary cell isolations



(Figure 6F,G, arrowheads indicate capillary-like networks). Collectively, these data underscore the role of IL-10 in stimulating angiogenesis-inducing factors by dermal fibroblasts and suggest that fibroblasts are a potential target cell for IL-10's pro-angiogenic effects.

### 3.8 | IL-10 enhanced wound re-epithelialization and capillary lumen density in db/db murine wounds

Our data from WT mice support our working postulate that overexpression of LV IL-10 upregulates VEGF and CXCL12, thereby promoting EPC-mediated neovascularization and wound healing. To assess the impact of this signaling under impaired wound healing conditions, we studied the effect of LV IL-10 overexpression in a db/db murine wound model of type II diabetes.

We pretreated dorsal skin in db/db mice with LV IL-10, wounding the skin after 4 days to allow transgenic protein overexpression, and then harvested these wounds at day 7 post-injury. Our results show that LV IL-10 overexpression significantly improved re-epithelialization in db/db wounds as compared to LV GFP or PBS treated controls (Figure 7A–D). Strikingly, while the granulation tissue area was bland and comprised predominantly of adipose tissue in the LV GFP and PBS controls, LV IL-10-treated wounds had a robust granulation tissue deposition (Figure 7E), similar in morphology to WT mice wounds. We then analyzed wound sections with MECA-32 staining and found a significant increase in capillary lumen density in LV IL-10-treated db/db wounds as compared to LV GFP or PBS controls (Figure 7F–I). Furthermore, a significant increase in the CD133+Flk1+ EPC levels in the wound beds was also observed in LV IL-10-treated db/db wounds as compared to LV GFP or PBS controls (Figure 7J–M), with a concomitant increase in VEGF and CXCL12 gene expression in the wounds (Figure 7N,O). Taken together, our data support the significance of IL-10 overexpression in improving standard wound healing parameters and in increasing the recruitment, survival, and retention of EPCs to promote vascular lumen density and tissue repair,

even under diabetic conditions in which wound healing is impaired.

## 4 | DISCUSSION

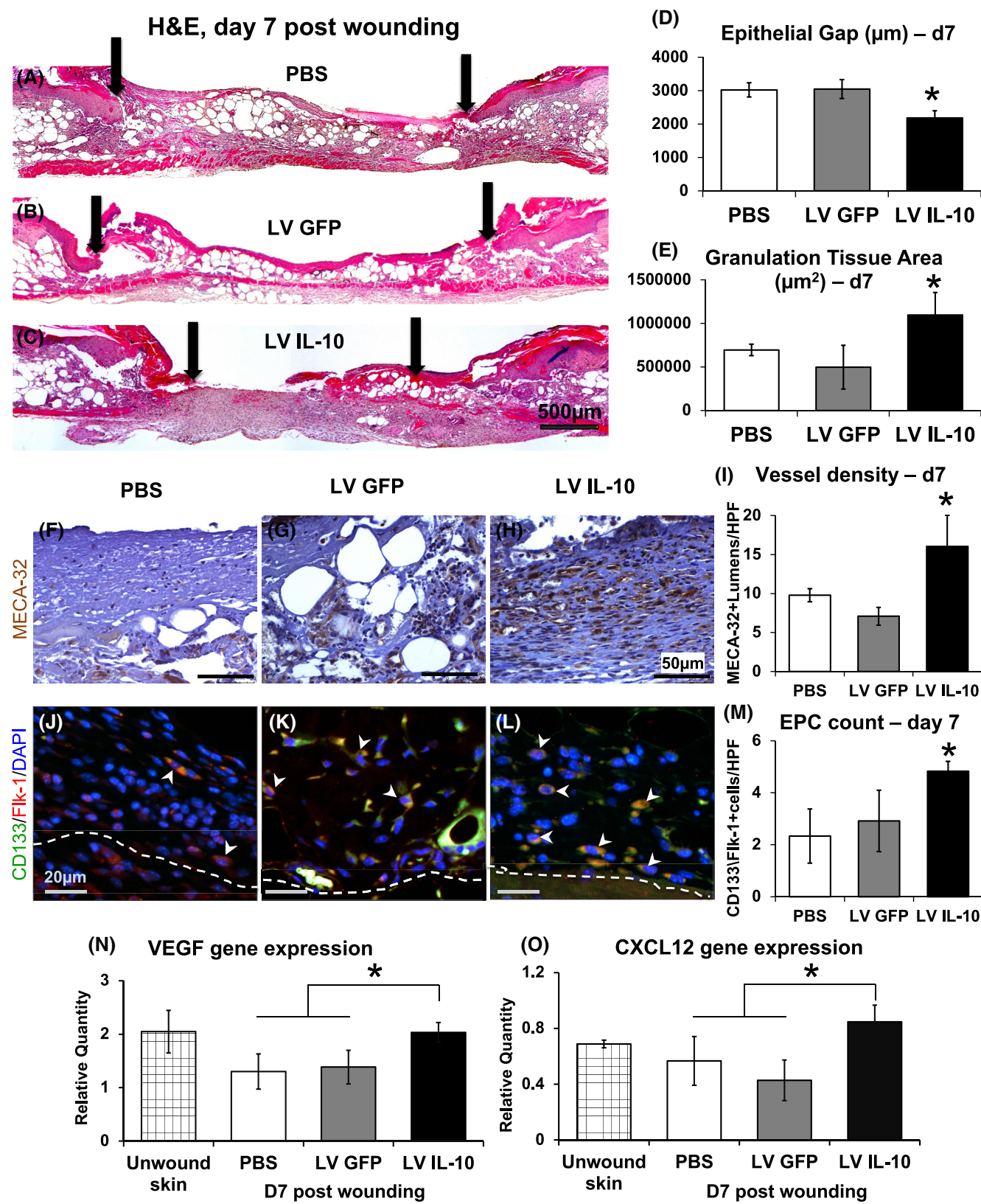
We show here that IL-10 overexpression can play a pivotal role in postnatal cutaneous wound neovascularization and healing in both normal and diabetic wounds. In addition to its well accepted role in immunoregulation and regenerative dermal wound repair, our data underscore a novel biological function for IL-10 in enhancing dermal wound vascular density by promoting EPC mobilization and recruitment. Our data support the capacity of IL-10 to induce EPC recruitment via VEGF and CXCL12 signaling. Therefore, we propose a model wherein IL-10 overexpression in cutaneous wounds increases the expression of VEGF and CXCL12 by fibroblasts at sites of dermal injury, resulting in a positive VEGF and CXCL12 gradient that favors mobilization of EPCs from the bone marrow, which can then home to injured tissues to support wound healing and neovascularization (Figure 8). These collective findings are also consistent with our working hypothesis that the IL-10 signaling cascade leading to enhanced wound neovascularization and healing is STAT3-dependent,<sup>55</sup> as IL-10's effects on wound capillary lumen density, angiogenic growth factor expression, and EPC levels were lost in the murine model of skin-specific STAT3 knockdown.

Importantly, our present study was also able to show the potential of IL-10 overexpression in significantly improving wound healing outcomes in diabetic mice, which included improved EPC recruitment and retention to the site of injury to promote wound capillary lumen density. In previous studies, the presence of unresolved inflammation in chronic wound environments has been suggested to impair EPC function and increase EPC apoptosis and elimination in the wound bed.<sup>61</sup> This phenomenon may partly explain why current strategies aimed at pharmacologically enhancing EPC mobilization from the BM, as well as ex vivo transplantation of expanded autologous EPCs<sup>62,63</sup> have not attained optimal efficacy in clinical trials. In this context, IL-10 may present a more effective

**FIGURE 7** IL-10 enhanced wound re-epithelialization and capillary lumen density in diabetic murine wound model. Dorsal wounds in db/db mice treated with either PBS, lentiviral GFP, or lentiviral IL-10 were harvested at 7 days post injury. (A–C) Hematoxylin and Eosin staining reveals that lentiviral IL-10 treated wounds re-epithelialize faster as compared to the two control groups. Quantitation of epithelial gap (D) and granulation tissue is shown (E). (F–H) Representative images of MECA-32 stained wounds section across the three treatment conditions—PBS, lentiviral GFP, or lentiviral IL-10 respectively. Increased MECA-32 stained-capillary lumens are seen in lentiviral IL-10 wounds, which is quantitatively significant (I). (J–M) Increase in the CD133+Flk1+ EPC levels in the wound beds is also observed in lentiviral IL-10-treated db/db wounds as compared to the control treatments. (N–O) qRT-PCR on wound tissue homogenates collected at day 7 shows that VEGF (N) and (O) CXCL12 expression is significantly higher lentiviral IL-10 treated cohort as compared to the PBS and lentiviral GFP controls. Scale bar = 500  $\mu$ m in (A–C), 50  $\mu$ m in (F–H) and 20  $\mu$ m in (J–L); Bar plots: mean  $\pm$  SD, 2 sections/wound,  $n = 4$  wounds from different mice/treatment group, \* $p < .05$  by ANOVA

strategy to both enhance EPC recruitment and increase the retention and numbers of these cells to participate in wound neovascularization in adverse microenvironments characterized by prolonged inflammation and

impaired wound healing such as in diabetic wounds, as it has the additional benefit of regulating inflammation. This strategy has been reported by Krishnamurthy et al., who demonstrated in a murine myocardial infarction (MI)





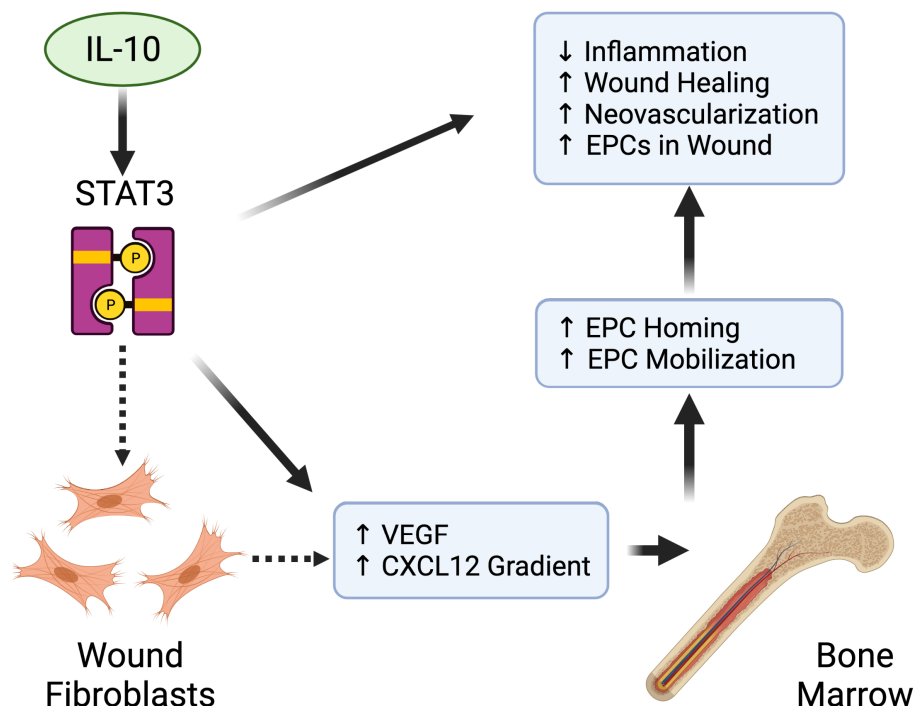


**FIGURE 8** IL-10 can play a pivotal role in postnatal cutaneous wound healing and neovascularization by influencing EPC mobilization and recruitment via STAT3-dependent increase in VEGF and CXCL12. IL10 overexpression, via a STAT3-dependent mechanism, results in enhanced levels of VEGF and CXCL12, wound healing, and neovascularization associated with an increase in EPCs in the wound. We put forth a potential pathway that IL-10 overexpression may induce wound fibroblasts to produce more VEGF and CXCL12, which creates a positive gradient for bone marrow derived EPC mobilization and homing to healing tissue. Image created using BioRender.com

model that treatment with IL-10 enhanced transplanted EPC association with vascular structures and their overall survival, resulting in improved neovascularization of the injured myocardium and left ventricular function. They further showed that IL-10 treatment enhanced STAT3 signaling and increased VEGF and CXCL12 expression in the myocardium after MI, providing mechanistic insights into IL-10's effects on EPCs.<sup>45</sup>

The present studies provide compelling evidence that treatment with IL-10 overexpression promotes VEGF expression in cutaneous wounds and establishes a positive CXCL12 concentration gradient that favors EPC mobilization from the bone marrow and homing to the site of injury, which could account for higher numbers of EPCs both in the peripheral blood and in wound microenvironment compared to baseline. Our *in vitro* data support dermal fibroblasts as one of the potential sources of IL-10-induced VEGF and CXCL12 in response to injury, a notion also supported by previous murine wound healing studies.<sup>44</sup> Furthermore, our data place CXCL12 upstream of IL-10-induced fibroblast VEGF signaling in the wound environment. In inflammatory environments, phosphorylated STAT3 is known to directly induce expression of VEGF, while also interacting with HIF-1 $\alpha$  to form a complex with CREB binding protein and p300, which in turn enhances expression of HIF-1 $\alpha$  target genes, including

VEGF.<sup>64,65</sup> Hypoxic conditions, noted in wounded skin damage of vasculature, also activate STAT3 to inhibit HIF-1 degradation via interaction with the C-terminal domain of HIF-1, thus preventing ubiquitination by Von Hippel-Lindau tumor suppressor protein (pVHL) and subsequent degradation.<sup>66,67</sup> While these mechanisms may explain how IL-10 STAT3 activation leads to wound VEGF expression, further research is needed to fully understand the mechanism behind the IL-10-associated increases in VEGF expression observed in the serum and BM compartments. Our studies also propose MMP9 as an intermediary in the IL-10-induced EPC mobilization cascade, but once again, focused future studies will be required to fully assess the contribution of MMP9 to the IL-10-VEGF-CXCL12 and EPC axis. These studies could provide relevant information that could eventually lead to innovative targeted therapies to optimize EPC mobilization, wound neovascularization, and regenerative wound healing. Cell types other than fibroblasts could also be involved in the effects reported here, and future efforts will be directed towards adapting our skin-specific STAT3 knockout model system to develop keratinocyte, fibroblast, or endothelial cell specific STAT3-deficient mice to study role of each of these cell types in IL-10 signaling.

We and others have shown that IL-10 overexpression regulates inflammatory responses and promotes regenerative

wound healing phenotype in murine cutaneous wounds in a dose-dependent manner.<sup>51–53</sup> Furthermore, we have recently reported a novel role for IL-10 in inducing a fibroblast-mediated formation of an extracellular wound matrix rich in hyaluronan,<sup>54</sup> which proved to be essential for IL-10's regenerative wound healing capability. In addition, IL-10 also regulates the synthesis and degradation of various extracellular matrix molecules in different fibroblastic cell types, which uphold anti-fibrotic effects of IL-10 in skin wound healing.<sup>68–70</sup> Yet, its impact on the process of cutaneous wound neovascularization in physiologic and pathophysiologic disease states such as diabetes has not been completely deciphered. Cutaneous wounds of IL-10<sup>−/−</sup> mice demonstrated an accelerated angiogenic response during the early phase (day 3) of wound healing, along with an increase in VEGF-A, with macrophages comprising the majority of VEGF-A expressing cells in the wounds.<sup>71</sup> Similar findings of an increase in angiogenic burst along with robust inflammation and rapid closure of wounds were reported in mice deficient in the expression of other chemokines, such as IL-12/23.<sup>72</sup> These studies suggest that IL-10-mediated inflammatory cytokine balance regulates angiogenic responses during dermal wound healing. Furthermore, IL-10-deficient EPCs express impaired migratory function *in vitro* in response to CXCL12. Such impairments in EPC function have also been noted in diabetic wound healing along with local deficiency in CXCL12 expression levels, specifically in myofibroblasts and keratinocytes, in the wounds.<sup>44</sup> While our studies support that IL-10 enhances cytokine production to favor EPC mobilization and recruitment, further inquiry must be undertaken to elucidate whether IL10 directly alters the biology of EPCs leading to their greater survival and function with roles in physiologic and constitutively inflamed tissues.

A limitation of this study is that we have examined only the CXCL12-VEGF pathway by which IL-10 promotes angiogenesis. Further studies on the roles of other growth factors and chemokine ligand-receptor interactions in promoting IL-10's effects on neovascularization must be conducted. For example, TGF- $\beta$  is a well-known regulator of angiogenesis, though its role is tissue dependent. In wound healing specifically, TGF- $\beta$ 1 is strongly pro-angiogenic, promoting endothelial cell migration and colony formation.<sup>73</sup> Similarly, TGF- $\beta$ 3, which beyond being anti-fibrotic, is also strongly pro-angiogenic,<sup>74</sup> and TGF- $\beta$ 3 expression in LV-treated wounds was highly increased. While we showed an increase in gene expression of CXCR4, a receptor for CXCL12, in whole wound tissue of LV IL-10 treated wounds, expression of CXCR4 present on immune and endothelial progenitor cells was not examined. Interaction between CXCR4 and CXCL12 is known to promote angiogenesis via the Akt signaling

pathway to promote VEGF expression.<sup>75</sup> Our findings showing abrogation in IL-10 induced VEGF in cultured fibroblasts with CXCL12 inhibition by antibody binding suggests that IL-10 may act via similar signaling pathways, and this should be explored further. Furthermore, while CXCL12 is the cognate ligand of CXCR4, other ligands, such as MIF,<sup>76,77</sup> an alternative ligand of CXCR4, have been demonstrated to have a role in EPC recruitment and wound healing, which needs to be further evaluated.

In summary, our data provide evidence that supports a role for IL-10 in enhancing VEGF and CXCL12 levels, EPC recruitment, and wound neovascularization, and ultimately improving cutaneous wound healing via STAT3 signaling. The immunoregulatory and anti-inflammatory effects of IL-10 may also serve to enhance EPC mobilization, survival, and function in the wounds. These data additionally point out the need to design precision strategies to deliver targeted and sustained levels of IL-10 with the therapeutic potential to enhance EPC-driven angiogenesis and wound healing in normal and diabetic wounds.

## ACKNOWLEDGEMENTS

The authors sincerely acknowledge the technical support received from our laboratory staff members and the support received from Cincinnati Children's Hospital Medical Center Flow Cytometry Core. The authors also acknowledge the editorial support of Drs. Monica Fahrenholtz and Hector Martinez-Valdez from the Office of Surgical Research Administration (OSRA), Department of Surgery, Texas Children's Hospital. This study is supported by 1R01GM111808NIH/NIGMS (SGK) and Wound Healing Society Foundation 3M Award (SB), and the John S. Dunn Foundation Collaborative Research Award Program administered by the Gulf Coast Consortia (SB).

## DISCLOSURES

The authors on the manuscript do not have any conflict of interest (either financial or personal).

## AUTHOR CONTRIBUTIONS

Swathi Balaji, Emily Steen, Timothy M. Crombleholme, Paul L. Bollyky, and Sundeep G. Keswani designed the experiments; Walker D. Short, Swathi Balaji, Aditya Kaul, Emily Steen, Xinyi Wang, Hima V. Vangapandu, Natalie Templeman, Alexander J. Blum, Chad M. Moles, Oluyinka O. Olutoye, performed bench and animal related experimental work; Walker D. Short, Swathi Balaji, Emily Steen, Xinyi Wang, Hima V. Vangapandu, Natalie Templeman, Alexander J. Blum, Chad M. Moles, Daria A. Narmoneva, Manish J. Butte, Timothy M. Crombleholme, Paul L. Bollyky, and Sundeep G. Keswani analyzed data; Walker D. Short, Swathi Balaji, Emily Steen, Xinyi Wang,

Hima V. Vangapandu, Natalie Templeman, Alexander J. Blum, Oluyinka O. Olutoye, Chad M. Moles, Daria A. Narmoneva, Timothy M. Crombleholme, Manish J. Butte, Paul L. Bollyky, and Sundeeep G. Keswani contributed to the discussions, manuscript writing and editing. We affirm that all authors have read and agree with the manuscript.

## DATA AVAILABILITY STATEMENT

The data that support the findings of this study are available in the methods and/or supplementary material of this article. Data sharing not applicable to this article as no datasets were generated or analyzed during the current study.

## ORCID

Swathi Balaji  <https://orcid.org/0000-0001-8875-8008>

## REFERENCES

- Economic costs of diabetes in the U.S. in 2017. *Diabetes Care*. 2018;41(5):917-928.
- Frykberg RG, Banks J. Challenges in the treatment of chronic wounds. *Adv Wound Care*. 2015;4(9):560-582.
- Casqueiro J, Casqueiro J, Alves C. Infections in patients with diabetes mellitus: a review of pathogenesis. *Indian J Endocrinol Metab*. 2012;16(Suppl 1):S27-S36.
- Balaji S, King A, Crombleholme TM, Keswani SG. The role of endothelial progenitor cells in postnatal vasculogenesis: implications for therapeutic neovascularization and wound healing. *Adv Wound Care*. 2013;2(6):283-295.
- Ribatti D, Vacca A, Nico B, Roncali L, Dammacco F. Postnatal vasculogenesis. *Mech Dev*. 2001;100(2):157-163.
- Asahara T, Masuda H, Takahashi T, et al. Bone marrow origin of endothelial progenitor cells responsible for postnatal vasculogenesis in physiological and pathological neovascularization. *Circ Res*. 1999;85(3):221-228.
- Urbich C, Dimmeler S. Endothelial progenitor cells: characterization and role in vascular biology. *Circ Res*. 2004;95(4):343-353.
- Tepper OM, Capla JM, Galiano RD, et al. Adult vasculogenesis occurs through in situ recruitment, proliferation, and tubulization of circulating bone marrow-derived cells. *Blood*. 2005;105(3):1068-1077.
- Carmeliet P. Developmental biology. One cell, two fates. *Nature*. 2000;408(6808):43-45.
- Ehrbar M, Metters A, Zammaretti P, Hubbell JA, Zisch AH. Endothelial cell proliferation and progenitor maturation by fibrin-bound VEGF variants with differential susceptibilities to local cellular activity. *J Control Release*. 2005;101(1-3):93-109.
- Urbich C, Aicher A, Heeschen C, et al. Soluble factors released by endothelial progenitor cells promote migration of endothelial cells and cardiac resident progenitor cells. *J Mol Cell Cardiol*. 2005;39(5):733-742.
- Patel J, Seppanen EJ, Rodero MP, et al. Functional definition of progenitors versus mature endothelial cells reveals key SoxF-dependent differentiation process. *Circulation*. 2017;135(8):786-805.
- Asahara T, Murohara T, Sullivan A, et al. Isolation of putative progenitor endothelial cells for angiogenesis. *Science*. 1997;275(5302):964-967.
- Peichev M, Naiyer AJ, Pereira D, et al. Expression of VEGFR-2 and AC133 by circulating human CD34(+) cells identifies a population of functional endothelial precursors. *Blood*. 2000;95(3):952-958.
- Falanga V. Wound healing and its impairment in the diabetic foot. *Lancet*. 2005;366(9498):1736-1743.
- Blakytyn R, Jude E. The molecular biology of chronic wounds and delayed healing in diabetes. *Diabet Med*. 2006;23(6):594-608.
- Phillips TJ. Chronic cutaneous ulcers: etiology and epidemiology. *J Invest Dermatol*. 1994;102(6):38S-41S.
- Kim KA, Shin YJ, Kim JH, et al. Dysfunction of endothelial progenitor cells under diabetic conditions and its underlying mechanisms. *Arch Pharm Res*. 2012;35(2):223-234.
- Capla JM, Grogan RH, Callaghan MJ, et al. Diabetes impairs endothelial progenitor cell-mediated blood vessel formation in response to hypoxia. *Plast Reconstr Surg*. 2007;119(1):59-70.
- Madonna R, De Caterina R. Cellular and molecular mechanisms of vascular injury in diabetes—part II: cellular mechanisms and therapeutic targets. *Vascul Pharmacol*. 2011;54(3-6):75-79.
- Callaghan MJ, Ceradini DJ, Gurtner GC. Hyperglycemia-induced reactive oxygen species and impaired endothelial progenitor cell function. *Antioxid Redox Signal*. 2005;7(11-12):1476-1482.
- Fadini GP, Miorin M, Facco M, et al. Circulating endothelial progenitor cells are reduced in peripheral vascular complications of type 2 diabetes mellitus. *J Am Coll Cardiol*. 2005;45(9):1449-1457.
- Keswani SG, Katz AB, Lim FY, et al. Adenoviral mediated gene transfer of PDGF-B enhances wound healing in type I and type II diabetic wounds. *Wound Repair Regen*. 2004;12(5):497-504.
- Tepper OM, Galiano RD, Capla JM, et al. Human endothelial progenitor cells from type II diabetics exhibit impaired proliferation, adhesion, and incorporation into vascular structures. *Circulation*. 2002;106(22):2781-2786.
- Vasa M, Fichtlscherer S, Aicher A, et al. Number and migratory activity of circulating endothelial progenitor cells inversely correlate with risk factors for coronary artery disease. *Circ Res*. 2001;89(1):E1-E7.
- Kalka C, Masuda H, Takahashi T, et al. Transplantation of ex vivo expanded endothelial progenitor cells for therapeutic neovascularization. *Proc Natl Acad Sci USA*. 2000;97(7):3422-3427.
- Suh W, Kim KL, Kim JM, et al. Transplantation of endothelial progenitor cells accelerates dermal wound healing with increased recruitment of monocytes/macrophages and neovascularization. *Stem Cells*. 2005;23(10):1571-1578.
- Balaji S, Vaikunth SS, Lang SA, et al. Tissue-engineered provisional matrix as a novel approach to enhance diabetic wound healing. *Wound Repair Regen*. 2012;20(1):15-27.
- Cho H, Balaji S, Sheikh AQ, et al. Regulation of endothelial cell activation and angiogenesis by injectable peptide nanofibers. *Acta Biomater*. 2012;8(1):154-164.
- Georgescu A, Alexandru N, Constantinescu A, Titorencu I, Popov D. The promise of EPC-based therapies on vascular dysfunction in diabetes. *Eur J Pharmacol*. 2011;669(1-3):1-6.
- Li B, Sharpe EE, Maupin AB, et al. VEGF and PlGF promote adult vasculogenesis by enhancing EPC recruitment and vessel formation at the site of tumor neovascularization. *FASEB J*. 2006;20(9):1495-1497.
- Asahara T, Takahashi T, Masuda H, et al. VEGF contributes to postnatal neovascularization by mobilizing bone

- marrow-derived endothelial progenitor cells. *EMBO J*. 1999;18(14):3964-3972.
33. Rosti V, Massa M, Campanelli R, De Amici M, Piccolo G, Perfetti V. Vascular endothelial growth factor promoted endothelial progenitor cell mobilization into the peripheral blood of a patient with POEMS syndrome. *Haematologica*. 2007;92(9):1291-1292.
  34. Heeschen C, Dimmeler S, Hamm CW, Boersma E, Zeiher AM, Simoons ML. Prognostic significance of angiogenic growth factor serum levels in patients with acute coronary syndromes. *Circulation*. 2003;107(4):524-530.
  35. Heissig B, Hattori K, Dias S, et al. Recruitment of stem and progenitor cells from the bone marrow niche requires MMP-9 mediated release of kit-ligand. *Cell*. 2002;109(5):625-637.
  36. Tang JM, Wang JN, Zhang L, et al. VEGF/SDF-1 promotes cardiac stem cell mobilization and myocardial repair in the infarcted heart. *Cardiovasc Res*. 2011;91(3):402-411.
  37. Sengupta N, Afzal A, Caballero S, et al. Paracrine modulation of CXCR4 by IGF-1 and VEGF: implications for choroidal neovascularization. *Invest Ophthalmol Vis Sci*. 2010;51(5):2697-2704.
  38. Peled A, Petit I, Kollet O, et al. Dependence of human stem cell engraftment and repopulation of NOD/SCID mice on CXCR4. *Science*. 1999;283(5403):845-848.
  39. Rey M, Valenzuela-Fernandez A, Urzainqui A, et al. Myosin IIA is involved in the endocytosis of CXCR4 induced by SDF-1alpha. *J Cell Sci*. 2007;120(Pt 6):1126-1133.
  40. Liu ZJ, Tian R, An W, et al. Identification of E-selectin as a novel target for the regulation of postnatal neovascularization: implications for diabetic wound healing. *Ann Surg*. 2010;252(4):625-634.
  41. Moore MA, Hattori K, Heissig B, et al. Mobilization of endothelial and hematopoietic stem and progenitor cells by adenovector-mediated elevation of serum levels of SDF-1, VEGF, and angiopoietin-1. *Ann N Y Acad Sci*. 2001;938:36-45; discussion 45-37.
  42. Hattori K, Heissig B, Tashiro K, et al. Plasma elevation of stromal cell-derived factor-1 induces mobilization of mature and immature hematopoietic progenitor and stem cells. *Blood*. 2001;97(11):3354-3360.
  43. Bauer SM, Bauer RJ, Liu ZJ, Chen H, Goldstein L, Velazquez OC. Vascular endothelial growth factor-C promotes vasculogenesis, angiogenesis, and collagen constriction in three-dimensional collagen gels. *J Vasc Surg*. 2005;41(4):699-707.
  44. Gallagher KA, Liu ZJ, Xiao M, et al. Diabetic impairments in NO-mediated endothelial progenitor cell mobilization and homing are reversed by hyperoxia and SDF-1 alpha. *J Clin Invest*. 2007;117(5):1249-1259.
  45. Krishnamurthy P, Thal M, Verma S, et al. Interleukin-10 deficiency impairs bone marrow-derived endothelial progenitor cell survival and function in ischemic myocardium. *Circ Res*. 2011;109(11):1280-1289.
  46. Losordo DW, Dimmeler S. Therapeutic angiogenesis and vasculogenesis for ischemic disease. Part I: angiogenic cytokines. *Circulation*. 2004;109(21):2487-2491.
  47. Cho H, Balaji S, Hone NL, et al. Diabetic wound healing in a MMP9-/- mouse model. *Wound Repair Regen*. 2016;24(5):829-840.
  48. Couper KN, Blount DG, Riley EM. IL-10: the master regulator of immunity to infection. *J Immunol*. 2008;180(9):5771-5777.
  49. Ouyang W, Rutz S, Crellin NK, Valdez PA, Hymowitz SG. Regulation and functions of the IL-10 family of cytokines in inflammation and disease. *Annu Rev Immunol*. 2011;29:71-109.
  50. Wang Y, Fan L, Meng X, et al. Transplantation of IL-10-transfected endothelial progenitor cells improves retinal vascular repair via suppressing inflammation in diabetic rats. *Graefes Arch Clin Exp Ophthalmol*. 2016;254(10):1957-1965.
  51. Peranteau WH, Zhang L, Muvarak N, et al. IL-10 overexpression decreases inflammatory mediators and promotes regenerative healing in an adult model of scar formation. *J Invest Dermatol*. 2008;128(7):1852-1860.
  52. Gordon A, Kozin ED, Keswani SG, et al. Permissive environment in postnatal wounds induced by adenoviral-mediated overexpression of the anti-inflammatory cytokine interleukin-10 prevents scar formation. *Wound Repair Regen*. 2008;16(1):70-79.
  53. Kieran I, Knock A, Bush J, et al. Interleukin-10 reduces scar formation in both animal and human cutaneous wounds: results of two preclinical and phase II randomized control studies. *Wound Repair Regen*. 2013;21(3):428-436.
  54. Balaji S, Wang X, King A, et al. Interleukin-10-mediated regenerative postnatal tissue repair is dependent on regulation of hyaluronan metabolism via fibroblast-specific STAT3 signaling. *FASEB J*. 2017;31(3):868-881.
  55. Moore KW, de Waal MR, Coffman RL, O'Garra A. Interleukin-10 and the interleukin-10 receptor. *Annu Rev Immunol*. 2001;19:683-765.
  56. Levy DE, Lee CK. What does Stat3 do? *J Clin Invest*. 2002;109(9):1143-1148.
  57. Hiramatsu K, Sasagawa S, Outani H, Nakagawa K, Yoshikawa H, Tsumaki N. Generation of hyaline cartilaginous tissue from mouse adult dermal fibroblast culture by defined factors. *J Clin Invest*. 2011;121(2):640-657.
  58. Baker M, Robinson SD, Lechertier T, et al. Use of the mouse aortic ring assay to study angiogenesis. *Nat Protoc*. 2011;7(1):89-104.
  59. Pfaffl MW. A new mathematical model for relative quantification in real-time RT-PCR. *Nucleic Acids Res*. 2001;29(9):e45.
  60. Morris LM, Klanke CA, Lang SA, et al. Characterization of endothelial progenitor cells mobilization following cutaneous wounding. *Wound Repair Regen*. 2010;18(4):383-390.
  61. Desouza CV, Hamel FG, Bidasee K, O'Connell K. Role of inflammation and insulin resistance in endothelial progenitor cell dysfunction. *Diabetes*. 2011;60(4):1286-1294.
  62. Ingram DA, Caplice NM, Yoder MC. Unresolved questions, changing definitions, and novel paradigms for defining endothelial progenitor cells. *Blood*. 2005;106(5):1525-1531.
  63. Fadini GP, Losordo D, Dimmeler S. Critical reevaluation of endothelial progenitor cell phenotypes for therapeutic and diagnostic use. *Circ Res*. 2012;110(4):624-637.
  64. Pawlus MR, Wang L, Hu CJ. STAT3 and HIF1alpha cooperatively activate HIF1 target genes in MDA-MB-231 and RCC4 cells. *Oncogene*. 2014;33(13):1670-1679.
  65. Zhou X, Yan T, Huang C, et al. Melanoma cell-secreted exosomal miR-155-5p induce proangiogenic switch of cancer-associated fibroblasts via SOCS1/JAK2/STAT3 signaling pathway. *J Exp Clin Cancer Res*. 2018;37(1):242.
  66. Jung JE, Kim HS, Lee CS, et al. STAT3 inhibits the degradation of HIF-1alpha by pVHL-mediated ubiquitination. *Exp Mol Med*. 2008;40(5):479-485.



67. Jung JE, Lee HG, Cho IH, et al. STAT3 is a potential modulator of HIF-1-mediated VEGF expression in human renal carcinoma cells. *FASEB J*. 2005;19(10):1296-1298.
68. Yamamoto T, Eckes B, Krieg T. Effect of interleukin-10 on the gene expression of type I collagen, fibronectin, and decorin in human skin fibroblasts: differential regulation by transforming growth factor-beta and monocyte chemoattractant protein-1. *Biochem Biophys Res Comm*. 2001;281(1):200-205.
69. Moroguchi A, Ishimura K, Okano K, Wakabayashi H, Maeba T, Maeta H. Interleukin-10 suppresses proliferation and remodeling of extracellular matrix of cultured human skin fibroblasts. *Eur Surg Res*. 2004;36(1):39-44.
70. Shi JH, Guan H, Shi S, et al. Protection against TGF-beta1-induced fibrosis effects of IL-10 on dermal fibroblasts and its potential therapeutics for the reduction of skin scarring. *Arch Dermatol Res*. 2013;305(4):341-352.
71. Eming SA, Werner S, Bugnon P, et al. Accelerated wound closure in mice deficient for interleukin-10. *Am J Pathol*. 2007;170(1):188-202.
72. Matias MA, Saunus JM, Ivanovski S, Walsh LJ, Farah CS. Accelerated wound healing phenotype in Interleukin 12/23 deficient mice. *J Inflamm*. 2011;8:39.
73. Evrard SM, d'Audigier C, Mauge L, et al. The profibrotic cytokine transforming growth factor-beta1 increases endothelial progenitor cell angiogenic properties. *J Thromb Haemost*. 2012;10(4):670-679.
74. Muraoka N, Shum L, Fukumoto S, Nomura T, Ohishi M, Nonaka K. Transforming growth factor-beta3 promotes mesenchymal cell proliferation and angiogenesis mediated by the enhancement of cyclin D1, Flk-1, and CD31 gene expression during CL/Fr mouse lip fusion. *Birth Defects Res A Clin Mol Teratol*. 2005;73(12):956-965.
75. Liang Z, Brooks J, Willard M, et al. CXCR4/CXCL12 axis promotes VEGF-mediated tumor angiogenesis through Akt signaling pathway. *Biochem Biophys Res Comm*. 2007;359(3):716-722.
76. Grieb G, Piatkowski A, Simons D, et al. Macrophage migration inhibitory factor is a potential inducer of endothelial progenitor cell mobilization after flap operation. *Surgery*. 2012;151(2):268-277.e261.
77. Emontzpohl C, Goetzenich A, Simons D, et al. Key role of MIF in the migration of endothelial progenitor cells in patients during cardiac surgery. *Int J Cardiol*. 2015;181:284-287.

## SUPPORTING INFORMATION

Additional supporting information may be found in the online version of the article at the publisher's website.

**How to cite this article:** Short WD, Steen E, Kaul A, et al. IL-10 promotes endothelial progenitor cell infiltration and wound healing via STAT3. *FASEB J*. 2022;36:e22298. doi:[10.1096/fj.201901024RR](https://doi.org/10.1096/fj.201901024RR)